NASA
Technical
Paper
2460

May 1985

Flow Rate and Pressure Profiles for One to Four Axially Alined Orifice Inlets

Robert C. Hendricks and
T. Trent Stetz

NASA

NASA Technical Paper 2460

1985

Flow Rate and Pressure Profiles for One to Four Axially Alined Orifice Inlets

Robert C. Hendricks and
T. Trent Stetz

Lewis Research Center
Cleveland, Ohio

NASA

National Aeronautics
and Space Administration

**Scientific and Technical
Information Branch**

Summary

Choked flow rate and pressure profile data were taken on sequential, axially alined inlets of the orifice type, with an l/d (orifice length-to-diameter ratio) of 0.5. The configuration consisted of two to four inlets spaced 0.66 and 32 orifice diameters apart.[1] Reference data were taken for the limiting case of a single orifice inlet. At a spacing of 32 diameters the reduced flow rate appeared to follow the simple power-law relation

$$\frac{G_r}{G_{r,1}} = N^{-b}$$

where $G_{r,1}$ is the reduced flow rate for a single inlet, N is the number of inlets, and b, although temperature dependent, is approximately 0.4. At this spacing the instrumented orifices and spacers gave pressure profiles that dropped sharply at the entrance and partially recovered within each inlet, somewhat independent of N. At low inlet temperatures jetting through the last orifice was common.

At a spacing of 0.66 diameter fluid jetting through all N inlets was prevalent at low temperatures for each configuration studied, as indicated by the flat pressure profiles and flow rates, which were nearly identical to those for a single orifice inlet.

A simplifying relation was developed between the friction loss parameters for flow through N sequential tubes and N sequential inlets. The predicted flow rates for N tubes were in reasonable agreement with the N-inlet analysis and followed the simple power-law relation given. Other relations derived from the N-inlet analysis were applied to the experimental flow rates with some success.

Introduction

Contoured inlet configurations are common to heat transfer devices and fluid machinery components. Most such inlet configurations consist of sequential inlets. Compressors, pin-finned heat exchangers, labyrinth and step seals, etc., are examples of inlet configurations consisting of two or more sequential inlets or, in a stricter sense, sequential flow development. The details of the flow dynamics and heat transfer in these configurations are in many cases not well understood. For example, in a study of seals for high-performance turbomachines (ref. 1) the flow appeared to separate and jet through the third-stage length in the maximum-clearance channel when the seal was placed in the fully eccentric position.

The unusual results of reference 1 instigated a series of choked fluid flow tests with single and multiple sharp-edge orifice and Borda inlets. These studies (refs. 2 to 8) demonstrate that such a jetting phenomenon could occur over a wide range of fluid state conditions. Flow jetting (refs. 2 to 4 and 6) was found to be inhibited by high reduced inlet stagnation temperatures ($T_{r,0}>1$) and to a lesser extent by low inlet stagnation pressure $P_{r,0}$. At high L/D, decreasing $P_{r,0}$ inhibits jetting. Furthermore, as inlet stagnation conditions approach saturation, jetting is limited to low L/D and usually does not occur for inlets with net quality greater than zero. Here L is the spacing between orifices. In flow jetting the metastable liquid-like jet tends toward reattachment because of the rapid vapor release and the tube roughness. These tests establish that jetting can occur in the single inlet orifice or Borda passage to over 105 L/D.

As a first look at discontinuities of sequential inlets (refs. 5, 7, and 8) the effects of using four sequential, axially alined orifice and Borda inlets were investigated. Water table flow visualization studies of these inlets indicated that for $L/D<1$ jetting could occur. For $L/D>20$ the flow appeared to be nearly independent of the previous sequential inlet. Flow instabilities were pronounced for the range $1<L/D<10$. Experimental tests of cryogenic fluids in four orifice and four Borda axially alined inlets demonstrated that for a spacing of nominally 30 L/D the flow was nearly independent of the upstream inlets and reservoirs but that jetting did occur in the fourth (or last) inlet at lower inlet stagnation temperatures. At a spacing of nominally 0.7 L/D, jetting through all of the inlets at the lower inlet temperatures was commonplace, and the flow appeared to be controlled at the first inlet independently of the configuration.

[1]Data for four sequential, axially alined orifice inlets for 32-diameter and 0.66-diameter spacings and with applied backpressure are found in NASA TP-1967.

Choked flow rate and pressure profile data for a configuration consisting of one to four Borda inlets were studied and the results presented in reference 9. These results again demonstrated that for the 30-diameter spacing the flow was independent of the upstream inlets, no matter how many (up to four) were studied. These results also demonstrated that at the 0.8-diameter spacing the sequential inlets acted as one inlet at the lower inlet stagnation temperatures for four, three, or two inlets. The data of reference 9 seem to follow a simple empirical relation:

$$\frac{G_r}{G_{r,1}} = N^{-b} \tag{1}$$

where b was found to be temperature dependent and nominally 0.4 for a range of test temperatures outside the thermodynamic critical region.

A few other studies on axially alined sequential inlets have been done, such as that of Boscole, Martin, and Donnis (ref. 10), who were mainly interested in the improvement of flowmeters. Benchert and Wachter (ref. 11) present a thorough study of the stability of see-through and leaved labyrinth seals. Iwatsubo (ref. 12) has also studied the stability of flows in labyrinth seal cavities. His results seem to be nearly the analytic complement to the experimental work of Benchert and Wachter (ref. 11). Komotori and Mori (ref. 13) studied the isentropic expansion of a perfect gas through labyrinth seals. These studies serve as limiting cases and guides to the experimentation and analysis presented herein.

In these latter references (refs. 10 to 13) the working-fluid states are either incompressible liquid or gas, and the range of fluid conditions usually encountered with cryogens, and in many high-performance turbomachines, is not considered. Single inlets (refs. 2 to 4 and 6), four sequential orifice and Borda inlets (refs. 5, 7, and 8), and two or more sequential Borda inlets (ref. 9) were studied over a range of inlet conditions and geometric arrangements. However, no correspondence has been made between two, three, four, or more sequential orifice inlets.

Consequently, the purpose of this report is to determine the nature of the flow rates and pressure distributions in N sequential orifice inlets at spacing of 0.66 and 32 diameters over a wide range of fluid state conditions. In this study we are limited to $N=4$.

Symbols

A area

b slope

C constant

C_d flow loss coefficient

C_f flow coefficient

c clearance

D diameter of inlet, or hydraulic diameter

d diameter

F function, see appendix

f friction factor

G mass flow rate

G^* flow normalizing parameter, 6010 g/cm^2 s for nitrogen

H enthalpy

ID inside diameter of sequential inlet

i i^{th} inlet

k_s rms roughness

L spacing

L_* equivalent length

l length of orifice inlet

M limiting number of inlets

m slope

N number of inlets

OD inside diameter of spacer tube

P pressure

R radius

R/k_s relative roughness

Re Reynolds number

S entropy

T temperature

u velocity

V specific volume

$\dot{w}$ weight flow

x length

β area ratio

ϵ roughness, related to k_s

ρ density, $1/V$

τ shear

μ viscosity

Subscripts:

c thermodynamic critical

e exit

I isentropic

i i^{th} sequential inlet, or axial coordinate position

in inlet

j axial coordinate position

k summation index

m	maximum
out	outlet
r	reduced by normalizing parameter
w	wall
0	stagnation or reference
1	case for $N=1$ (single inlet), or unit equivalent tube
+	reference length

Apparatus and Instrumentation

The flow facility (fig. 1), a blowdown type, was basically that described in references 14 and 9, but modified to accommodate the sequential orifice inlet configurations. The working fluid was nitrogen.

Orifice inlets with l/D of 0.5, where l is the length of the orifice inlet, were designed to be similar to those used in reference 3, with spacers of 15.24 and 0.32 cm (6.0 and 0.125 in.). This provided two fixed spacings of 32 and 0.66 diameter, respectively.

The N-sequential-orifice-inlet configuration with 0.32-cm (0.125-in.) spacers is illustrated schematically in figure 2(a), which also provides details of the orifice inlet geometry and pressure tap locations. Details of the orifice inlet are shown in figure 3. A schematic of the N-sequential-orifice-inlet configuration with 15.24-cm (6.0-in.) spacers, shown in figure 2(b), also gives the pressure tap locations on these spacers.

The configuration was fitted between inlet and outlet flange adapters to accommodate the multiple lengths. The multiple surfaces were satisfactorily sealed against the pressure-to-vacuum environment by thin Mylar gaskets between the flat faces. The test section installation is shown in figure 4.

The pressure data were recorded as described in references 5, 7, and 14. Again, the working fluid was nitrogen and the reduced temperature range was $0.68<T_{r,0}<2.5$ (liquid to gas), with reduced pressure to $P_{r,0}<2.5$.

Analysis

The treatment of the simplest set of sequential inlets is quite complicated. The analysis herein will be broken into four sections: (1) the thermodynamic process path and governing equations, (2) the relation between N inlets and one inlet, (3) the relation between N tubes and N inlets, and (4) the relation between friction loss parameter and flow coefficient.

Thermodynamic Process Path and Governing Equations

Sequential expansions are complicated processes and are quite difficult to assess either experimentally or theoretically. In a thermodynamic treatment, where only the end state conditions are considered, the sequential inlet problem is assumed to be adiabatic, that is, to consist of a series of isentropic expansions across each inlet followed by an isobaric recovery in a "mixing chamber" or spacer to the adiabatic locus (fig. 5). This procedure is quite similar to the approach given by Komotori and Mori (ref. 13) for flow through labyrinth seals.

The governing equations, described in reference 5, can be written (fig. 5) as

$$\left(\frac{G}{C_f}\right)_i^2 = 2\rho^2(H_0 - H_i) \tag{2}$$

where the subscript i represent the i^{th} inlet, with the following constraints:
Isentropic

$$S_0(P_0,T_0)\Big|_i = S(P_e,T_e)\Big|_i \tag{3}$$

Isobaric

$$P_{e,i} = P_0\Big|_{i+1} \tag{4}$$

Critical flow (choked)

$$G_m^2\left(\frac{dV}{dP}\right)_e\Bigg|_{i=N} = -1 \tag{5}$$

where

$$G_m^2 = \left(\frac{2}{V^2}\right)\int_P^{P_0} V\,dP\Big|_{i=N} \tag{6}$$

Upon convergence, G approaches G_m. Equations (5) and (6) are evaluated at the N^{th} (or last) inlet.

The solution of these equations, although straightforward, is quite difficult and some elementary first-order approximations, as discussed later, are needed. To determine a solution, each inlet must be independent of the previous inlet, and we must assume (1) the pressure ratio across the first inlet, (2) that the choking condition applies to the last inlet, (3) that the iteration will converge to a solution, and (4) a flow coefficient for each inlet. A constant flow coefficient of 0.75 was assumed to account for entrance losses of each inlet with low carryover to the next sequential reservoir and inlet in order to expedite the development of a solution. Fluid properties were calculated by using GASP (ref. 15).

Convergence problems were encountered when applying these governing equations to flows near the critical region. However, the flows above and below the critical region, $T_{r,0}<0.9$ and $T_{r,0}>1.1$ for a range in pressure seemed to be somewhat well described by these

equations. At the last inlet, $i=N$, low pressures and those near saturation may necessitate the use of a separate nonequilibrium model that allows a certain degree of metastability, which appears to be important for these pressures. The nonequilibrium model may better represent the flows in these regions as demonstrated in references 5 and 7. The results are discussed in the penultimate section.

At the 0.66-diameter spacing it was assumed that the flow recognizes the N-inlet configuration as one inlet because of the jetting condition at this spacing. This assumption was based on previous experimental results and flow visualization studies, which were limited to four sequential inlets.

Elementary Relation of N-Inlets to One Inlet

The flow rates in sequential inlets can also be analyzed by extrapolating the flow rate through a single inlet with the appropriate constraints. The flow rate through the i^{th} inlet can be approximated by a modified Bernoulli equation:

$$\dot{w}2 = \left[\frac{(2C_f^2A^2\Delta P)}{V}\right]_i \tag{7}$$

and since

$$\Delta P = P_0\left(1-\frac{P_e}{P_0}\right) = \sum_{i=1}^{N}\Delta P_i \tag{8}$$

the flow rate can be rewritten as

$$\dot{w}2 = \frac{P_0\left(1-\frac{P_e}{P_0}\right)}{R} \tag{9}$$

where

$$R = \sum_{i=1}^{N}\left[\frac{V}{2C_f^2A^2}\right]_i \tag{10}$$

If $V/(2C_f^2A^2)$ is nearly constant for each sequential inlet,

$$R \approx N\left[\frac{V}{2C_f^2A^2}\right]_{i=1} \tag{11}$$

Let $\dot{w}_1$ be characterized by

$$\dot{w}_1 = \left[\frac{2C_f^2A^2}{V}\right]_{i=1}\left[P_0\left(1-\frac{P_e}{P_0}\right)\right] \tag{12}$$

Then it follows that

$$\frac{\dot{w}}{\dot{w}_1} = N^{-m} \tag{13}$$

and for constant areas

$$\frac{G_r}{G_{r,1}} = N^{-m} \qquad \text{where } m = 1/2 \tag{14}$$

Thus, knowing the mass flow rate (or flux) in one inlet, we can determine the flow rate through any number of N inlets. Although this assumes that the N inlets act independently of each other and furthermore that the losses per stage are the same for each sequential inlet, it provides a good approximation.

Elementary Relation Between N Tubes and N Inlets

N inlets and N tubes can be related by making use of friction factors and flow coefficients. Figure 6 and reference 16 show how the ratio of the mass flow rate to the ideal flow rate of an isentropic fluid is related to the friction loss parameter $4fL/D$ for flows in constant-area ducts. The limiting slope in figure 6 appears to be $-1/2$, with a range of $-1/3 > m > -1/2$, for some $4fL/D$ greater than $(4fL/D)_0 \sim 1$. For this section of the plot

$$\frac{G_r}{G_{r,I}} \propto \left(\frac{4fL}{D}\right)^{-m} \tag{15}$$

Now if the total friction factor loss is the sum of the individual "tube" friction factor losses and furthermore each "tube" loss is the same,

$$\frac{4fL}{D} = \sum_{i=1}^{N}\left(\frac{4fL}{D}\right)_i \approx N\left(\frac{4fL}{D}\right)_i \tag{16}$$

where i refers to a unit tube of diameter D, length L, and equivalent friction factor f, which is based on Reynolds number and surface roughness. Thus

$$\frac{G_r}{G_{r,I}} \propto N^{-m}\left(\frac{4fL}{D}\right)_i^{-m} \tag{17}$$

In the plots of reference 9 and herein it is apparent that the flow rates in the sequential inlets can be described by

$$\frac{G_r}{G_{r,1}} \propto N^{-m} \tag{18}$$

For $N=1$ and $G_{r,1}=G_{r,I}C_f$, the ratio of flow rates becomes

$$\frac{G_r}{G_{r,I}} \propto C_f N^{-m} \tag{19}$$

Then it follows that

$$\left(\frac{4fL}{D}\right)_i^{-m} = C_f \tag{20}$$

This is a good approximate relationship between N tubes and N inlets. For a more complete characterization of the application to sequential inlets, based on the governing equations cited previously, see the appendix.

Relation Between Friction Loss Parameter and Flow Coefficient

To use the friction loss parameter $4fL/D$ in the analysis of sequential inlets, one needs to develop a relation between the friction loss parameter and the flow coefficient. For sequential inlets we assume the equivalent "sand" surfaces to be characterized as fully rough, that is, independent of Reynolds number. From the Moody charts

$$\frac{1}{\sqrt{4f}} = 2.07 \log_{10}\left(\frac{R}{k_s}\right) + 0.99 \tag{21}$$

and from Schlichting (ref. 17)

$$\frac{1}{\sqrt{4f}} = 2 \log_{10}\left(\frac{R}{k_s}\right) + 1.74 \tag{22}$$

where R/k_s is the relative roughness.

It is clear from previous work (refs. 5 and 7) that C_f is not constant but depends on temperature and to a lesser extent on pressure. For the isentropic flow of a gas (ref. 21)

$$G_{r,I}\left(\frac{\sqrt{T_{r,0}}}{P_{r,0}}\right) = \text{Constant} \approx \frac{1}{5} \tag{23}$$

and since $G_r/G_{r,I}=C_f$

$$G_r\left(\frac{\sqrt{T_{r,0}}}{P_{r,0}}\right) = G_{r,I}\left(\frac{\sqrt{T_{r,0}}}{P_{r,0}}\right) C_f = \frac{C_f}{5} \tag{24}$$

For the more complex fluid case one would use the generalized flow charts of reference 19. For liquids and gases an equivalent friction factor can probably be found. However, for the fluid states in between, C_f and hence the friction factor vary considerably.

As an example of how one might use the previous results to determine the developed flow regime, consider four orifices ($N=4$) at the nominal spacing of 30 diameters (refs. 5 and 7). For liquids and gases C_f values are nearly constant.

$$(C_f)_{N=1} \begin{cases} = 0.37 \text{ liquid} \\ = 0.52 \text{ gas} \end{cases} \tag{25}$$

Thus, since $(4fL/D) \approx C_f^{-2}$, then $4fL/D$ is 7.3 for the liquid and 3.7 for the gas. For a fully roughened condition $4fL/D$ is the same for both.

Assume that

$$\frac{R}{k_s} = \frac{\text{OD} - \text{ID}}{\text{ID}} \tag{26}$$

for the experimental system. Realizing that the L/D of the experimental system must somehow enter into the definition of R/k_s, then $R/k_s=3$ and $4f=0.256$ from the Moody equation. Thus L/D becomes 28.5 for the liquid and 14.4 for the gas. The experimental L/D is 32, and thus either case can be classified as fully rough.

Friction, surface roughness, or equivalent "sand" roughness will become an important factor with the sequential orifice inlets spaced at 0.66 diameter. At this spacing the sequential inlets are assumed to act as a single inlet (ref. 7) with $4fL/D < (4fL/D)_0$ (the reference value), that is when the equivalent friction loss parameter per tube is small. As the number of inlets increases at this spacing, the friction loss parameter increases, and the slope of the plot begins to deviate from a small value at the point where the sequential inlets spaced at 0.66 diameter should cease to act as a single inlet. Hence there should exist a limiting $N=M$ where equivalent roughness will become a strong factor (ref. 2). Figure 6 and reference 16 may be applicable here.

Thus the sequential inlets can be thought to act like a sequence of connected tubes with various amounts of friction present.

Results

Experimental Results

The experimental results covering a wide range of temperatures and pressures are presented here in two sections: flow rates, and pressure profiles. The experimental flow rate and pressure profile data are presented in tables I to VIII, where tables VII and VIII are representative sample sets. A complete set of tables VII and VIII are available in reference 7.

Flow rates.—Reduced flow rate as a function of reduced inlet stagnation pressure at selected isotherms is presented in figure 7. The reduced flow rate is given by

$$G_r = \frac{G}{G^*} \tag{27}$$

where G^* is determined by the extended corresponding states theory (refs. 5 and 20 to 22).

The flow rates for two to four sequential orifice inlets at a spacing of 32 diameters (figs. 7(a) to (c), respectively) showed similar trends. The flow rate profiles for a single orifice are given in figure 1(d). At the 0.66-diameter spacing the flow rates for two to four sequential orifice inlets (figs. 7(e) to (g)) had similar trends. These flow rates were substantially higher than those of the 32-diameter spacing but, again, corresponded in form and magnitude to those of a single orifice inlet (fig. 7(d)).

Flow rates for selected temperatures and pressures as a function of N at the 32-diameter spacing are given in figure 8. The plotted flow rates for the experimental data were determined from the "smoothed" curves of figures 7(a) to (d). The slopes b were calculated by using the least-squares technique. They seemed to vary with reduced temperature and slightly with reduced pressure.

Pressure profiles.—The variation of pressure profile with inlet stagnation temperature is shown in figure 9. As the spacing changed from 0.66 diameter to 32 diameters, there was a drastic change in the pressure profile.

At the 32-diameter spacing (figs. 9(b) to (d)) the pressure profiles exhibited somewhat of a sharp drop at the entrance of each inlet and recovered very slightly within the spacer chamber. The two to four sequential orifices exhibited similar trends, with the single inlet as a reference comparison (fig. 9(a)). At the lower inlet stagnation temperatures the pressure profiles were flat at the last inlet, an indication of jetting as in references 1 to 3, 5, 7, and 8. The pressure recovery varied the most in the last inlet at this spacing. Jetting occurred at the lower inlet stagnation temperatures, but the higher inlet temperatures exhibited an arched profile at the last inlet.

At the 0.66-diameter spacing (figs. 9(e) to (g)) the pressure profile at the lower inlet stagnation temperatures resembled that of a free jet. The fluid seemed to flow unimpeded through the sequential inlets, even though they were separated by a 0.66-diameter spacer. At the higher inlet stagnation temperatures the sharp drop at the first inlet was followed by a recovery, somewhere between that of a free jet and that of the sequential inlets spaced at 32 diameters.

Further comparisons and other data can be found in references 1 to 3, 5, 7, and 8, including some effects of backpressure.

Analytic Comparisons

We expected that the 32-diameter-spaced inlets would act independently of each other. The constant flow coefficient used to predict the flow rates caused some problems. In addition, problems were also encountered when trying to calculate flows near the thermodynamic critical region.

The calculated flow rates for liquid and gas for two to four sequential inlets approximated the experimental curves fairly well. The calculated flow rates for the liquid, $T_{r,0}=0.68$, always were higher than the experimental flow rates. This characteristic has been previously encountered in references 4 and 22 to 24. The theoretical flow rates for the gas are usually close to the experimental values. The calculated curve for four sequential orifices fit the data better than did the calculated curve for two sequential orifices. The assumption of a constant flow coefficient of 0.75 was not correct even though it could be used to describe the four-sequential-inlet case reasonably well. We assumed a constant value for C_f in our effort to make a unified comparison.

Mass flux of N Inlets.—Figure 8 compares the experimental flow rates with the calculated flow rates for N sequential inlets at the 32-diameter spacing. The experimental and calculated flow rates seemed to follow an empirical power-law relation:

$$G_r \propto N^{-b} \tag{28}$$

where N is the number of inlets and b is an undetermined function of inlet stagnation temperature and pressure.

Flow rates have been calculated for up to 20 sequential inlets for gas, but the data are limited to the four inlets of this experiment. The seal of reference 1 contained a stepped labyrinth flow path of 33 teeth, which can be thought of as 33 sequential inlets. The general configuration for gas flow studies is also illustrated in reference 18. The calculated flow rates for $N \leq 20$ gave an exponent b of 0.43 for gas (nominally 0.4). Plotting the reduced flow rates versus N for calculated values to $N=20$ and some of the experimental labyrinth seal data at $N=33$ when corrected for carryover showed fairly good agreement with the empirical power-law relation (fig. 10).

From the experimental results as well as the theoretical calculations it appeared that $b \approx 0.4$; from the elementary

relation the expected value was $b \approx 0.5$. However, the value of 0.4 appeared to be valid, to a first approximation, over a wide range of reduced inlet pressures and temperatures, excluding the thermodynamic critical region.

Further normalizing the reduced mass flow rate by flow through a single inlet yields

$$\frac{G_r}{G_{r,1}} = N^{-b} \tag{1}$$

Thus, if $G_{r,1}$, the mass flux for a single inlet, and b are known, the mass flow rate for N well-separated, similar sequential inlets[2] over the same extensive range of $P_{r,0}$ and $T_{r,0}$ follows directly. Furthermore the mass flow rate is governed by the inlet stagnation conditions of the first inlet and N may be thought of as the inlet where choking occurs. That is, for example if choking occurs at the first inlet, $i = N = 1$. The effects of variable spacing have yet to be investigated.

Variations in exponent b.—The exponent b as a function of reduced inlet stagnation temperature is given in figure 11 for various reduced pressures. The exponent appeared to exhibit "sine" or variational behavior with respect to temperature. The amplitude of the variation of the exponent with reduced inlet temperature seemed to be less for reduced inlet pressures above the critical region than for those inlet pressures below the critical region. Behavior in the critical region is unknown. In the absence of information, figure 11 can be used to determine $b(T_{r,0})$, or $b(T_{r,0})$ can be taken as a constant ($b \sim 0.4$).

The experimental flow rates where the reduced inlet temperature $T_{r,0}$ is less than 1 had exponents whose magnitude was greater than that for flows above the critical region (i.e., where $T_{r,0} > 1$, fig. 8). An exponent of greater magnitude indicates a lower flow rate. Hence, as the temperature increased from below critical to above critical, the flow coefficient should have increased, as was illustrated in reference 7 for $N = 4$.

The calculated flows had a similar tendency in the exponents. The inlets separated by 32 diameters were assumed to act independently of each other for the purposes of finding an analytical result. However, there might have been some carryover effects due to the possible alinement of the flow at the lower inlet stagnation temperatures. This would decrease the magnitude of the exponent from that calculated at the lower temperatures.

Although the experimental exponents of the flow rates generally lay below the theoretical and losses were not accounted for in the theoretical analysis, both the calculated and experimental exponents were of a similar form with respect to their dependence on temperature. Until further investigations are completed, the flow rate and b are empirical functions of temperature, and figure 11 can be used as a guide.

The exponent b as a function of reduced pressure for various reduced temperatures is illustrated in figure 12. The exponent appeared in general to have a weak inverse linear dependence on pressure. Again the theoretical values were higher than the experimental values, except near the critical region (i.e., where $T_{r,0} = 0.9$). Calculating the flow rates for the gas to within reasonable accuracy was also difficult. For $T_{r,0} > 1$, the slope appeared to decrease with an increase in pressure and would probably do so until the limiting case where the N sequential inlets became equivalent to a rough tube.

Mass flux related to N tubes.—From equations (20) and (25) the friction loss parameter $4fL/D$ was found to be 7.3 and 3.7 for $N = 4$ for liquids and gases, respectively. If the inlets were assumed to act independently, then from equation (16), $4fL/D$ for $N = 1$ would be 1.83 for liquids and 0.83 for gases. From figure 6 and reference 16, $\dot{w}/\dot{w}_I$ (or C_f) was approximately 0.62 for liquids and approximately 0.72 for the gases. The data gave a value of 0.6 for liquid and 0.9 for gas. These compare reasonably well. Table IX shows a comparison between $\dot{w}/\dot{w}_I$ and $G_r/G_{r,I}$ (data) for various inlet temperatures and pressures. The data compare reasonably well with the values from figure 6 and reference 16. Hence the relation developed from N tubes is somewhat applicable to N sequential inlets.

Summary of Results

Choked flow rate and pressure profile data were taken and studied for up to four sequential orifice inlets for spacings of 32 and 0.66 diameter as an indicator of fluid flow through N sequential inlets.

At a spacing of 32 diameters the pressure profiles exhibited a sharp drop at the leading edge of the inlet followed by some recovery within the inlet and little recovery in the spacer chamber. At the lower inlet stagnation temperatures, fluid jetting occurred in the last of the sequential inlets. These sequential inlet configurations appeared to function independently with control (choking) at the last inlet ($i = N$).

At a spacing of 0.66 diameter fluid jetting was prevalent throughout all of the sequential inlets at the lower inlet stagnation temperatures. The flow rates were the same as for a single inlet and appeared to be controlled (choked) at the first inlet ($i = 1$) independently of the downstream configuration.

Analytic modeling is complex, but a simplistic model of the 32-diameter spacing appeared to give good

[2]The separation is 32 L/D for the geometries herein and 30 L/D for those in ref. 9 but is in general cavity geometry and Reynolds number dependent.

correlation with the experimental data outside of the thermodynamic critical region. The data seemed to follow a simple empirical relation

$$\frac{G_r}{G_{r,1}} = N^{-b}$$

where b is function of temperature and weakly dependent on pressure and is nominally 0.4. The principal feature of these results is that if one knows the mass flow rate for a single inlet, one knows, to a first order, the mass flow rate for N sequential inlets. Furthermore the mass flow rate is governed by the stagnation pressure and temperature conditions upstream of the first inlet.

A simple relation between N tubes and N inlets was developed as well as one for N inlets and one inlet. Estimations for flow rates using the N-tube friction factor model compared reasonably well with the experimental data.

Lewis Research Center
National Aeronautics and Space Administration
Cleveland, Ohio, April 25, 1984

Appendix—Relations Between N tubes and N inlets

Governing Equations

If we start with the one-dimensional momentum equation

$$-A\,dP-\tau_w\,dA_w=\dot{w}\,du$$

and use the definitions of friction factor and hydraulic diameter

$$f=\frac{\tau_w}{\frac{\rho u^2}{2}}, \qquad D=\frac{4A}{\frac{dA_w}{dx}}$$

the momentum equation becomes

$$-dP-\frac{4f\dot{w}}{2\rho A^2}\frac{dx}{D}=\frac{\dot{w}}{A}\,du$$

By substituting continuity and specific volume, $u=\dot{w}/\rho A$ and $V=1/\rho$, the momentum equation can be integrated to give the mass flow rate, or mass flux,

$$\left(\frac{\dot{w}}{A_j}\right)^2=G_j^2=\frac{\frac{-2}{V_j^2}\int_{P_i}^{P_j}V\,dP}{1-\left[\frac{\left(\frac{V}{A}\right)_i}{\left(\frac{V}{A}\right)_j}\right]^2+\left(\frac{A}{V}\right)_j^2\int_{P_i}^{P_j}\frac{4f}{D}\left(\frac{V}{A}\right)^2\frac{dx}{dP}\,dP}$$

where i and j refer to any two axial coordinate positions.

For the incompressible or nearly incompressible case (V=constant), the mass flow rate becomes

$$\dot{w}^2=\frac{2A_j^2\rho(P_i-P_j)}{1-\beta^2+A_j^2\int_{P_i}^{P_j}\frac{4f}{DA^2}\frac{dx}{dP}\,dP}$$

where β is the area ratio

$$\beta\equiv\frac{\left(\frac{V}{A}\right)_i}{\left(\frac{V}{A}\right)_j}$$

If we assume discrete steps where average values of f, D, and A can be used,

$$\dot{w}^2=\frac{2A_j^2\rho(P_i-P_j)}{1-\beta^2+A_j^2\left[\sum_k\frac{4f_k}{D_kA_k^2}\left(\frac{\Delta x}{\Delta P}\right)_k\Delta P_k\right]}$$

Since the numerator represents the ideal flow rates, the flow coefficient becomes

$$C_f^{-2}=\left(\frac{\dot{w}_I}{\dot{w}}\right)^2=1-\beta^2+A_j^2\left[\sum_k\frac{4f_k}{D_kA_k^2}\left(\frac{\Delta x}{\Delta P}\right)\Delta P_k\right]$$

$$\approx 1-\beta^2+\sum_k\frac{4f_k\Delta x_k}{D_k}\left(\frac{A_j}{A_k}\right)^2$$

Suppose now that we require the losses in a constant-area duct to be the same as those in a multiple-geometry duct, discussed by Wyler (ref. 25), and define

$$\frac{4f_0L_*}{D_0}\equiv\sum_k 4f_k\left(\frac{\Delta x_k}{D_k}\right)\left(\frac{A_j}{A_k}\right)^2$$

where L_* represents an equivalent length. Now $4f$ can be represented by a variety of friction laws such as those shown in table X, using pipe flow for the example. Equivalent values for sharp-edge entrance effects can also be cast in terms of $4f\Delta x/D$. Consider a simple power-law variation with Reynolds number (e.g., Blasius) as $f^{-1}\propto \mathrm{Re}^n$, and then divide it into developed flow terms and inlet (or undeveloped) flow terms:

$$L_*=L_{*,1}+L_{*,2}\equiv\sum_k\left(\frac{f_k}{f_0}\right)\left(\frac{D_0}{D_k}\right)\left(\frac{A_j}{A_k}\right)^2\Delta x_k$$

For the components with developed flows and constant properties

$$f\propto \mathrm{Re}^{-n}, \qquad \mathrm{Re}\propto\frac{d}{A}, \qquad f\propto\left(\frac{d}{A}\right)^{-n}$$

$$L_{*,1}=\sum_k\left(\frac{D_0}{D_k}\right)^{n+1}\left(\frac{A_0}{A_k}\right)^{n-2}\Delta x_k$$

For the components with undeveloped flows (again in the form of an adiabatic expansion)

$$\frac{4f\Delta x}{D} = F(C_f)$$

and

$$\frac{4f_0\Delta x_+}{D_0} = F(C_{f,0})$$

and the equivalent length becomes

$$L_{*,2} = \sum_k \left(\frac{4f\Delta x}{D}\right)_k \left(\frac{D_0}{4f_0\Delta x_+}\right) \left(\frac{A_0}{A_k}\right)^2 \Delta x_+$$
$$= \sum \frac{F(C_{f,k})}{F(C_{f,0})} \left(\frac{A_0}{A_k}\right)^2 \Delta x_+$$

where $A_j = A_0$ and where the function $F(C_f)$ can be approximated by the friction choke relation for an isentropic gas

$$\log_{10} F = \sqrt{\frac{-\log_{10} C_f}{c}} - 2$$

where

$C_f > 0.8$ $\qquad c = 0.03$

$0.56 \le C_f \le 0.8$ $\qquad c = 0.014F + 0.022$

$C_f \le 0.56$ $\qquad c = 0.05$

Also for a constant-area duct of length Δx_0, area A_0, friction factor f_0, and no inlet losses,

$$L_{*,0} = \Delta x_0$$

the ratio of developed terms becomes

$$\frac{L_{*,1}}{L_{*,0}} = \sum_k \left(\frac{D_0}{D_k}\right)^{n+1} \left(\frac{A_k}{A_0}\right)^{n-2} \left(\frac{\Delta x_k}{\Delta x_0}\right)$$

and the ratio of undeveloped terms becomes

$$\frac{L_{*,2}}{L_{*,0}} = \sum_k \frac{F_k}{F_0} \left(\frac{A_0}{A_k}\right)^2 \left(\frac{\Delta x_+}{\Delta x_0}\right)$$

Note that for large values of $F = (4fx/D)$, such as for a fully rough case,

$$C_{f,i}^{-2} \propto \left(\frac{4f\Delta x}{D}\right)_i$$

and

$$\frac{L_{*,2}}{L_{*,0}} = \sum \left(\frac{C_{f,0}}{C_{f,k}} \frac{A_0}{A_k}\right)^2 \frac{\Delta x_+}{\Delta x_0}$$

Thus the loss coefficient becomes

$$C_d^{-2} = 1 - \beta^2 + \left(\frac{L_*}{L_{*,0}}\right) \left(\frac{4f_0 L_{*,0}}{D_0}\right)$$

where

$$L_* = L_{*,1} + L_{*,2}$$

An interesting case follows when inlet effects are small, that is, $L_{*,2} \to 0$ and thus $L_* \to L_{*,1}$, where $L_{*,1}$ represents the equivalent length of the developed terms such as may exist in some types of seals (see development in ref. 25). It appears that in some sense $(L_*/L_{*,0})$ is a loss optimization factor. So also for incompressible flows

$$\beta = \frac{\left(\frac{V}{A}\right)_i}{\left(\frac{V}{A}\right)_j} \quad \to \frac{A_j}{A_i} \to \frac{A_0}{A_i}$$

and so C_d becomes for $f = C/\mathrm{Re}^n$,

$$C_d^{-2} = 1 - \left(\frac{A_0}{A_i}\right)^2 + \frac{4CL_{*,0}}{\mathrm{Re}_0^n D_0} \left(\frac{L_{*,1}}{L_{*,0}}\right)$$

The losses depend on β, L_{*1}, Re, and the reference geometry. For $\beta < 1$ (i.e., convergent geometry) the losses increase; for $\beta > 1$ (i.e., divergent geometry) the losses decrease.

The losses always increase with $L_*/L_{*,0}$. Usually A_0/A_i is sufficiently convergent and we therefore look at $L_*/L_{*,0}$. For a seal

$$D = \frac{4A}{P} = \mathrm{OD} - \mathrm{ID} = 2c$$

$$\frac{A_k}{A_0} \sim \frac{c_k(\mathrm{OD} + \mathrm{ID})_k}{c_0(\mathrm{OD} + \mathrm{ID})_0}$$

and for many connected or sequential seals

$$\frac{A_k}{A_0} \approx \frac{c_k}{c_0}$$

Thus

$$\frac{L_{*,1}}{L_{*,0}} \approx \sum \left(\frac{c_0}{c_k}\right)^{n+1} \left(\frac{c_k}{c_0}\right)^{n-2} \frac{\Delta x_k}{\Delta x_0} = \sum \left(\frac{c_0}{c_k}\right)^3 \frac{\Delta x_k}{\Delta x_0}$$

For selected seal passages or sequential inlets with constant clearance ratios

$$\frac{L_{*,1}}{L_{*,0}} \to \sum \frac{\Delta x_k}{\Delta x_0}$$

Furthermore for $(c_0/c_k) < 1$ (i.e., convergent flow passage) $L_{*,1}/L_{*,0}$ decreases and for $(c_0/c_k) > 1$ (i.e., divergent flow passage) $L_{*,1}/L_{*,0}$ increases. These results show just how sensitive seal leakage is to clearance ratios as the losses are linear in axial length $\Delta x_k/\Delta x_0$ but cubic in clearance ratio c_0/c_k.

Since sharp-edge inlets such as orifices and Borda inlets can usually be assigned a flow coefficient that is linear in $\Delta x_k/\Delta x_0$, the clearance ratio appears to remain the most significant factor in seal or sequential inlet leakage. This does not mean that one can in any way ignore the effects of the inlet. However, it must be remembered that leakage through any hole is a strong function of area.

Examples

Consider a convergent three-step seal configuration with constant clearance. The real inlet approach angle is 30° (i.e., not a sharp-edge (90°) inlet), and the two internal steps are full flow reversals. The fluid is nitrogen with inlet conditions as follows:

$$P_{r,0} = 1, \qquad P_{r,0} = \frac{P_0}{P_c}, \qquad P_c = 3.417 \text{ MPa}$$

$$T_{r,0} = 0.67, \qquad T_{r,0} = \frac{T_0}{T_c}, \qquad T_c = 126.3 \text{ K}$$

The reduced flow rate is

$$G_r = \frac{G}{G^*} = 0.41, \qquad G^* = 6010 \text{ g/cm}^2 \text{ s } (85.3 \text{ lbm/in}^2 \text{ s})$$

$$G = \rho u$$

and the average clearance for each step is

$$2c = D = 0.0254 \text{ cm } (0.010 \text{ in.})$$

For these values the Reynolds number becomes

$$\text{Re} = \frac{GD}{\mu} = \frac{(0.41)(6010)(0.0254)}{0.11 \times 10^{-2}} = 56\,900$$

The friction factors are about constant at

$$f_1 = \frac{0.0791}{\text{Re}^{1/4}} = 0.0051, \qquad f_2 \sim 0.0052, \qquad f_3 \sim 0.0053$$

The internal geometry of the seal gives unequal Δx and unequal cross-sectional areas

$$\Delta x_1 = 1.910 \text{ cm } (0.76 \text{ in.}) \qquad A_1 = 0.3166 \text{ cm}^2 (0.04907 \text{ in}^2)$$

$$\Delta x_2 = 1.384 \text{ cm } (0.545 \text{ in.}) \qquad A_2 = 0.3131 \text{ cm}^2 (0.04853 \text{ in}^2)$$

$$\Delta x_3 = 1.156 \text{ cm } (0.455 \text{ in.}) \qquad A_3 = 0.3075 \text{ cm}^2 (0.04766 \text{ in}^2)$$

Here A_3 is the control area, called A_0 in the analysis. Summing the friction terms gives

$$0.0053\left(\frac{0.76}{0.01}\right)\left(\frac{0.3075}{0.3166}\right)^2 + 0.0057\left(\frac{0.545}{0.01}\right) \times \left(\frac{0.3075}{0.3131}\right)^2 + 0.0051\left(\frac{0.455}{0.01}\right)\left(\frac{0.3075}{0.3075}\right)^2 = 0.91$$

and the developed flow loss coefficient becomes

$$\sum_k \frac{4 f_k \Delta x_k}{D_k}\left(\frac{A_0}{A_k}\right)^2 = 3.65 = \frac{4 f_0 L_{*,1}}{D_0}$$

For full flow reversals and $C_f = 0.6$

$$\log_{10} F = \sqrt{\frac{-\log_{10} C_f}{0.014F + 0.02}} - 2 \to F = 1.65$$

For a 30° inlet and $C_f = 0.8$

$$\log_{10} F = \sqrt{\frac{-\log_{10} C_f}{0.03}} - 2 \to F = 0.63$$

The flow coefficients for the undeveloped geometries (i.e., the inlet) and the full flow reversals give the following friction loss parameters:

$$\sum F_k \left(\frac{A_0}{A_k}\right)^2 = 0.63\left(\frac{0.3075}{0.3166}\right)^2 + 1.65\left(\frac{0.3075}{0.3131}\right)^2 + 1.65 = 3.8$$

The total loss coefficient becomes

$$C_d^{-2} = 1 - \beta^2 + \sum_k \frac{4f_k \Delta x_k}{D_k} \left(\frac{A_0}{A_k}\right)^2$$

$$= 1 - \left(\frac{0.3075}{0.3166}\right)^2 + 3.65 + 3.8$$

$$= 7.5 \rightarrow C_d = 0.36$$

which compares with 0.34 from the data when corrected for carryover.

Consider the same seal but with gas flows and the following inlet parameters:

$$P_{r,0} = 1, \qquad T_{r,0} = 2.3, \qquad G_r = 0.07$$

The Reynolds number is about the same as for the liquid, so one would not expect much of a change in the developed terms.

$$\mathrm{Re} = \frac{GD}{\mu} = \frac{(0.07)(6010)(0.0254)}{0.18 \times 10^{-3}} = 59\ 400$$

For full flow reversals and $C_f = 0.75$

$$\log_{10} F = \sqrt{\frac{-\log_{10} C_f}{0.014\,\mathrm{F} + 0.022}} - 2 \rightarrow F = 0.85$$

For a 30° inlet and $C_f = 0.85$

$$\log_{10} F = \sqrt{\frac{-\log_{10} C_f}{0.03}} - 2 \rightarrow F = 0.35$$

For the undeveloped terms the flow coefficients are increased and

$$\sum_k F_k \left(\frac{A_0}{A_k}\right)^2 = 0.35 \left(\frac{0.3075}{0.3166}\right)^2 + 0.85 \left(\frac{0.3075}{0.3131}\right)^2 + 0.85 = 2.0$$

Thus the undeveloped contribution is reduced and the loss coefficient becomes

$$C_d^{-2} = 1 - \beta^2 + \sum \left(\frac{4f\Delta x}{D}\right)_k \left(\frac{A_0}{A_k}\right)^2$$

$$= 1 - \left(\frac{0.3075}{0.3166}\right)^2 + 3.44 + 2.0$$

$$= 5.5 \rightarrow C_d = 0.43$$

This compares with 0.5 for the data, again corrected for carryover.

The equivalent length of a straight bore seal becomes

for liquids

$$L_* = \frac{(3.44+3.8)(0.0254)}{(4)(0.0051)} = 9\,\text{cm}\,(3.55\,\text{in.})$$

for gases

$$L_* = \frac{(3.44+1.98)(0.0254)}{(4)(0.0051)} = 6.7\,\text{cm}\,(2.7\,\text{in.})$$

The length of the three-step seal, in this example, is approximately 4.47 cm (1.76 in.)

$$L_{*,0} = 4.47\,\text{cm}\,(1.76\,\text{in.})$$

and thus the seal effectiveness becomes

for liquids

$$\frac{L_*}{L_{*,0}} = \frac{3.55}{1.76} = 2$$

for gases

$$\frac{L_*}{L_{*,0}} = \frac{2.7}{1.76} = 1.5$$

Now if we use the second approach

$$\left[\frac{L_{*,1}}{L_{*,0}}\right]_2 = \sum_k \left(\frac{D_0}{D_k}\right)^{n+1} \left(\frac{A_x}{A_0}\right)^{n-2} \left(\frac{\Delta x_k}{\Delta x_0}\right)$$

$$= \left(\frac{0.76}{1.76}\right)\left(\frac{0.3075}{0.3166}\right)^{1.75} + \left(\frac{0.545}{1.76}\right)\left(\frac{0.3075}{0.3131}\right)^{1.75} + \left(\frac{0.453}{1.76}\right)$$

$$= 0.97$$

and recall from the calculations that

$$\sum_k \left(\frac{4f\Delta x}{D}\right)_k \left(\frac{A_0}{A_k}\right)^2 = 3.44 = \frac{4f_0 L_{*,1}}{D_0}$$

and the ratio becomes

$$\left[\frac{L_{*,1}}{L_{*,0}}\right]_1 = \left(\frac{D_0}{4f_0}\right)\left(\frac{3.44}{1.76}\right) = \frac{0.01}{(4)(0.0051)}\left(\frac{3.44}{1.76}\right) = 0.96$$

The ratios are the same, but computation did not require evaluation of f except that the exponent n was assumed (necessary in either case).

In this example, the convergence is for stability considerations and detracts from seal leakage. The seal performance parameter or effective length comes from the "sequential inlets." In most cases, inlet effects cannot be ignored.

References

1. Hendricks, R. C.: A Comparison of Flow Rates and Pressure Profiles for *N*-Sequential Inlets and Three Related Seal Configurations. NASA TM-83442, 1983.
2. Hendricks, R. C.: Some Aspects of a Free Jet Phenomena to 105 *L/D* in a Constant Area Duct. Presented at 15th International Congress of Refrigeration (Venice, Italy), Sept. 23-29, 1979.
3. Hendricks, R. C.: A Free Jet Phenomena in a 90-Degree Sharp Edge Inlet Geometry. Presented at International Cryogenic Engineering Conference and International Cryogenic Materials Conference (Madison, Wis.), Aug. 21-24, 1979.
4. Hendricks, R. C.; and Poolos, N. P.: Critical Mass Flux Through Short Borda Type Inlets of Various Cross Sections. Proceedings of 15th International Congress of Refrigeration. Vol. II, 1980, pp. 73-77.
5. Hendricks, R. C.; and Stetz, T. T.: Some Flow Phenomena Associated with Aligned, Sequential Apertures with Borda Type Inlets—Inlet Pressure and Flow Separation. NASA TP-1792, 1981.
6. Hendricks, R. C.; and Simoneau, R. J.: Some Flow Phenomena in a Constant Area Duct with a Borda Type Inlet Including the Critical Region. NASA TM-78943, 1978.
7. Hendricks, R. C.; and Stetz, T. T.: Flow Through Aligned Sequential Orifices Type Inlets. NASA TP-1967, 1982.
8. Hendricks, R. C.; and Stetz, T. T.: Flow Through Axially Aligned Sequential Apertures of the Orifice and Borda Types. NASA TM-81681, 1981.
9. Hendricks, R. C.; and Stetz, T. T.: Flow Rate and Pressure Profiles for One to Four Axially Aligned Borda Type Inlets. NASA TP-2390, 1984.
10. Boscole, Robert A.; Martin, John M.; and Dennis, William E.: An Investigation of Fluid Flow Through Orifices in Series. MS Thesis, MIT, 1949.
11. Benckert, H.; and Wachter, J.: Flow Induced Spring Coefficients of Labyrinth Seals for Applications in Rotor Dynamics. Rotordynamic Instability Problems in High-Performance Turbomachinery. NASA CP-2133, 1980.
12. Iwatsubo, T.: Evaluation of Instability Forces of Labyrinth Seals in Turbines or Compressors. Rotordynamic Instability Problems in High-Performance Turbomachinery. NASA CP-2133, 1980.
13. Komotori, K.; and Mori, H.: Leakage Characteristics of Labyrinth Seals. Proceedings of 5th International Conference on Fluid Sealing. British Hydromechanics Research Association, 1971, pp. E4-45 through E4-63.
14. Hendricks, R. C.; et al.: Experimental Heat-Transfer Results for Cryogenic Hydrogen Flowing in Tubes at Subcritical and Supercritical Pressures to 800 Pounds per Square Inch Absolute. NASA TN D-3095, 1966.
15. Hendricks, R. C.; Baron, A. K.; and Peller, I. C.: GASP—A Computer Code for Calculating the Thermodynamic and Transport Properties for Ten Fluids: Parahydrogen, Helium, Neon, Methane, Nitrogen, Carbon Monoxide, Oxygen, Fluorine, Argon, and Carbon Dioxide. NASA TN D-7808, 1975.
16. Shapiro, Ascher H: The Dynamics and Thermodynamics of Compressible Fluid Flow, Vol. I. Ronald Press, 1953, p. 175.
17. Schlichting, Hermann: Boundary Layer Theory. McGraw Hill, 1960.
18. Hendricks, R. C.: Some Flow Characteristics of Conventional and Tapered High-Pressure-Drop Simulated Seals. ASME-ASLE Lubrication Conference (Dayton, Ohio), Oct. 16-18, 1979.
19. Simoneau, R. J.; and Hendricks, R. C.: Generalized Charts for Computation of Two-Phase Choked Flow of Simple Cryogenic Liquids. Cryogenics, vol. 17, no. 2, Feb. 1977, pp. 73-76.
20. Hendricks, R. C.: Normalizing Parameters for the Critical Flow Rate of Simple Fluids Through Nozzles. Proceedings of Fifth International Cryogenic Engineering Conference, K. Mendelssohn, ed., IPC Science and Technology Press, 1974, pp. 278-281.
21. Hendricks, R. C.; and Sengers, J. V.: Application of the Principle of Similarity to Fluid Mechanics. Presented at 9th International Conference on the Properties of Steam (Munich, West Germany), Sept. 8-14, 1979. (Also as NASA TM-79258, 1979.)
22. Hendricks, R. C.; Simoneau, R. J.; and Barrows, R.F.: Two-Phase Choked Flow of Subcooled Oxygen and Nitrogen Through Convergent-Divergent Nozzles. NASA TN D-8169, 1976.
23. Simoneau, R. J.; and Hendricks, R. C.: Two-Phase Choked Flow of Cryogenic Fluids in Converging-Diverging Nozzles. NASA TP-1484, 1979.
24. Simoneau, R. J.: Depressurization and Two-Phase Flow of Water Containing High Levels of Dissolved Nitrogen Gases. NASA TP-1839, 1981.
25. Wyler, J.S.: Design and Testing of a New Double Labyrinth Seal. ASME Paper 81-Lub-58. ASME/ASLE Joint Lubrication Conf., New Orleans, LA, Oct. 5-7, 1981.

TABLE I. - DATA FOR ONE ORIFICE INLET WITH A 32-DIAMETER SPACING TUBE AT EXIT

[Dimensions are in centimeters (inches).]

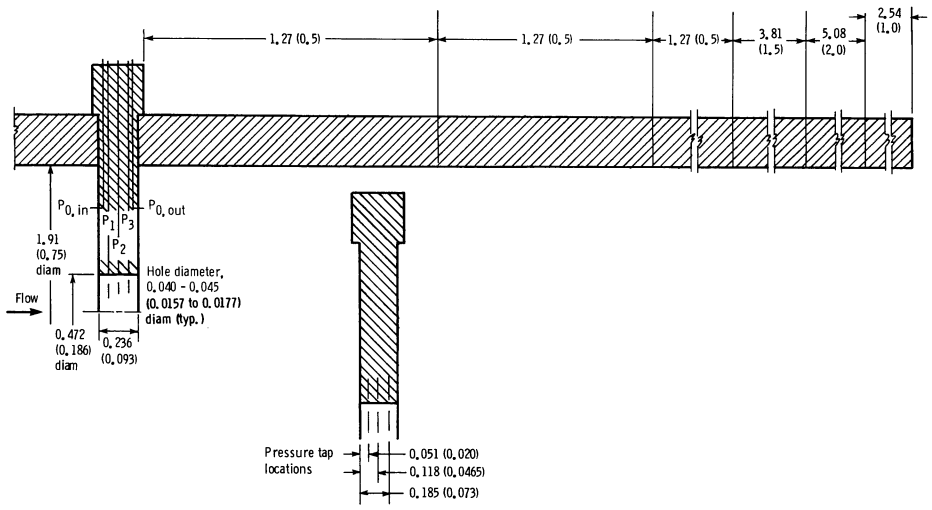

XRUN	MASS FLOW G/S	TIN K	PIN MPA	PBACK MPA	PR	GR	TR
ORIFICE INLET		POIN MPA	P1 MPA	P2 MPA	P3 MPA	POUT MPA	
			PN1	PN2	PN3	PN4	PN5
3315	33.3	260.0	0.896	0.000	0.262	0.031	2.059
	1	0.86	0.14	0.30	0.32	0.15	
		0.15	0.14	0.18	0.19	0.19	
3316	57.3	260.0	1.519	0.000	0.445	0.053	2.059
	1	1.49	0.24	0.48	0.54	0.18	
		0.17	0.16	0.21	0.24	0.25	
3317	85.0	259.0	2.217	0.000	0.649	0.079	2.051
	1	2.20	0.35	0.68	0.78	0.22	
		0.21	0.20	0.24	0.31	0.33	
3318	132.0	264.0	3.439	0.000	1.006	0.123	2.090
	1	3.43	0.58	1.04	1.19	0.30	
		0.30	0.29	0.34	0.45	0.48	
3319	186.0	265.0	4.826	0.000	1.412	0.173	2.098
	1	4.83	0.79	1.44	1.66	0.40	
		0.40	0.39	0.44	0.61	0.66	
3320	920.0	85.8	5.070	0.000	1.484	0.855	0.679
	1	5.00	0.13	0.12	0.11	0.13	
		0.11	0.00	0.15	0.16	0.23	
3321	823.0	85.9	4.010	0.000	1.174	0.765	0.680
	1	3.95	0.00	0.00	0.10	0.00	
		0.00	0.00	0.15	0.14	0.19	
3322	695.0	86.2	2.950	0.000	0.863	0.646	0.683
	1	2.89	0.10	0.11	0.11	0.10	
		0.00	0.00	0.15	0.12	0.18	
3323	587.0	85.7	2.170	0.000	0.635	0.546	0.679
	1	2.12	0.14	0.14	0.14	0.13	
		0.13	0.12	0.15	0.13	0.15	
3324	496.0	85.8	1.625	0.000	0.476	0.461	0.679
	1	1.58	0.17	0.16	0.16	0.13	
		0.15	0.14	0.16	0.16	0.17	
3325	412.0	86.0	1.217	0.000	0.356	0.383	0.681
	1	1.17	0.19	0.18	0.18	0.18	
		0.17	0.16	0.18	0.18	0.20	
3326	795.0	114.2	5.221	0.000	1.528	0.739	0.904
	1	5.17	0.65	0.63	0.63	0.63	
		0.62	0.60	0.62	0.71	0.86	
3327	686.0	113.7	4.026	0.000	1.178	0.638	0.900
	1	3.98	0.60	0.58	0.58	0.58	
		0.58	0.56	0.58	0.65	0.74	
3328	554.0	117.3	3.113	0.000	0.911	0.515	0.929
	1	3.06	0.65	0.64	0.67	0.60	
		0.59	0.64	0.62	0.68	0.71	
3329	326.0	115.9	2.000	0.000	0.585	0.303	0.918
	1	1.98	0.96	0.95	1.03	0.39	
		0.42	0.42	0.45	0.46	0.47	
3330	253.0	113.8	1.804	0.000	0.528	0.235	0.901
	1	1.78	1.04	1.05	1.05	0.30	
		0.30	0.33	0.43	0.38	0.39	
3331	780.0	115.1	5.119	0.000	1.498	0.725	0.911
	1	5.07	0.68	0.66	0.66	0.65	
		0.65	0.62	0.68	0.74	0.88	
3332	686.0	114.7	4.092	0.000	1.198	0.638	0.908
	1	4.04	0.62	0.61	0.60	0.60	
		0.60	0.58	0.60	0.67	0.77	
3333	554.0	114.5	2.887	0.000	0.845	0.515	0.907
	1	2.84	0.57	0.55	0.55	0.55	
		0.55	0.53	0.55	0.60	0.65	
3334	264.0	114.2	1.833	0.000	0.536	0.245	0.904
	1	1.80	1.03	1.04	1.06	0.32	
		0.32	0.35	0.39	0.40	0.40	
3335	637.0	127.0	5.460	0.000	1.598	0.592	1.006
	1	5.44	1.44	1.49	1.59	0.73	
		0.69	0.71	0.78	0.94	0.97	
3336	438.0	127.0	4.127	0.000	1.208	0.407	1.006
	1	4.12	1.76	1.84	1.91	0.51	
		0.50	0.55	0.61	0.69	0.71	
3337	247.0	126.6	3.355	0.000	0.982	0.230	1.002
	1	3.35	1.33	1.50	1.45	0.35	
		0.34	0.36	0.43	0.50	0.53	
3338	199.0	125.8	2.994	0.000	0.876	0.185	0.996
	1	2.98	0.82	1.28	1.29	0.28	
		0.27	0.28	0.34	0.42	0.44	
3339	205.0	127.0	3.075	0.000	0.900	0.191	1.006
	1	3.06	0.84	1.33	1.33	0.28	
		0.28	0.29	0.35	0.43	0.45	
3340	101.0	128.3	1.678	0.000	0.491	0.094	1.016
	1	1.65	0.30	0.54	0.59	0.19	
		0.18	0.18	0.22	0.27	0.28	

TABLE I. - Concluded.

XRUN	MASS FLOW G/S	TIN K	PIN MPA	PBACK MPA	PR	GR	TR
ORIFICE	INLET	POIN MPA	P1 MPA	P2 MPA	P3 MPA	POUT MPA	
		PN1	PN2	PN3	PN4	PN5	
3341	428.0	141.4	5.649	0.000	1.653	0.398	1.120
	1	5.66	1.45	2.06	2.47	0.54	
		0.53	0.58	0.68	0.82	0.84	
3342	295.0	141.3	4.422	0.000	1.294	0.274	1.119
	1	4.41	0.95	1.66	1.80	0.38	
		0.38	0.41	0.49	0.61	0.62	
3343	150.0	141.8	2.593	0.000	0.759	0.139	1.123
	1	2.57	0.43	0.83	0.91	0.25	
		0.24	0.24	0.29	0.37	0.38	
3344	97.4	143.5	1.768	0.000	0.517	0.091	1.136
	1	1.75	0.30	0.56	0.62	0.19	
		0.19	0.18	0.29	0.27	0.28	
3345	70.3	141.9	1.309	0.000	0.383	0.065	1.124
	1	1.28	0.23	0.41	0.45	0.17	
		0.16	0.15	0.19	0.22	0.23	
3346	670.0	84.3	2.717	0.000	0.795	0.623	0.667
	1	2.66	0.13	0.13	0.13	0.13	
		0.11	0.00	0.14	0.12	0.15	
3347	649.0	84.9	2.748	0.000	0.804	0.603	0.672
	1	2.70	0.30	0.28	0.29	0.35	
		0.34	0.32	0.37	0.51	0.52	

TABLE II. - DATA FOR TWO SEQUENTIAL, AXIALLY ALINED ORIFICE INLETS - 0.66-DIAMETER SPACING

[Dimensions are in centimeters (inches).]

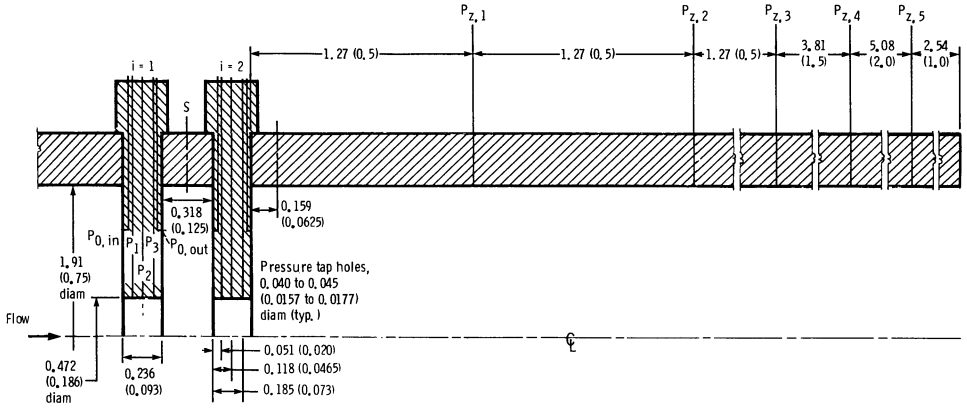

XRUN	MASS FLOW G/S	TIN K	PIN MPA	PBACK MPA	PR	GR	TR
ORIFICE INLET			POIN MPA	P1 MPA	P2 MPA	P3 MPA	POUT MPA
			PN1	PN2	PN3	PN4	PN5
3730	38.6	238.9	0.984	0.000	0.288	0.036	1.892
	1		0.97	0.18	0.30	0.39	0.48
	2		0.48	0.44	0.42	0.40	0.16
			0.13	0.13	0.15	0.18	0.22
3731	64.1	244.2	1.634	0.000	0.478	0.060	1.933
	1		1.62	0.29	0.48	0.67	0.83
	2		0.82	0.72	0.71	0.67	0.20
			0.17	0.17	0.20	0.24	0.28
3732	94.2	250.9	2.425	0.000	0.710	0.088	1.987
	1		2.42	0.45	0.71	1.00	1.24
	2		1.24	1.04	1.03	1.00	0.25
			0.22	0.64	0.26	0.33	0.37
3733	125.8	255.7	3.254	0.000	0.952	0.117	2.025
	1		3.26	0.60	0.95	1.38	1.69
	2		1.69	1.40	1.37	1.38	0.30
			0.27	0.29	0.33	0.43	0.47
3734	155.6	260.2	4.053	0.000	1.186	0.145	2.060
	1		4.06	0.80	1.18	1.71	2.09
	2		2.08	1.74	1.70	1.65	0.36
			0.32	0.35	0.40	0.52	0.57
3735	193.2	266.5	5.080	0.000	1.487	0.180	2.110
	1		5.09	1.03	1.49	2.13	2.58
	2		2.58	2.17	2.13	2.05	0.44
			0.40	0.43	0.50	0.64	0.70
3736	766.3	84.3	3.466	0.000	1.014	0.712	0.667
	1		3.42	0.11	0.12	0.11	0.12
	2		0.12	0.14	0.13	0.14	0.16
			0.13	0.13	0.14	0.15	0.24
3737	619.0	83.8	2.315	0.000	0.677	0.575	0.663
	1		2.28	0.00	0.11	0.00	0.10
	2		0.10	0.12	0.11	0.11	0.13
			0.10	0.10	0.11	0.11	0.17
3738	512.0	84.2	1.653	0.000	0.484	0.476	0.667
	1		1.61	0.12	0.12	0.11	0.12
	2		0.12	0.13	0.12	0.13	0.14
			0.12	0.12	0.13	0.13	0.18
3739	422.1	84.3	1.193	0.000	0.349	0.392	0.667
	1		1.16	0.13	0.14	0.13	0.14
	2		0.14	0.15	0.14	0.14	0.16
			0.13	0.14	0.14	0.14	0.20

XRUN	MASS FLOW G/S	TIN K	PIN MPA	PBACK MPA	PR	GR	TR
ORIFICE INLET			POIN MPA	P1 MPA	P2 MPA	P3 MPA	POUT MPA
			PN1	PN2	PN3	PN4	PN5
3740	721.1	115.4	4.413	0.000	1.291	0.670	0.914
	1		4.38	0.53	0.53	0.52	0.52
	2		0.52	0.56	0.57	0.59	0.63
			0.60	0.59	0.61	0.69	0.83
3741	548.0	114.3	2.782	0.000	0.814	0.509	0.905
	1		2.75	0.50	0.49	0.48	0.49
	2		0.49	0.52	0.53	0.53	0.55
			0.52	0.52	0.53	0.57	0.66
3742	489.8	114.0	2.324	0.000	0.680	0.455	0.903
	1		2.29	0.48	0.45	0.46	0.47
	2		0.47	0.50	0.50	0.50	0.52
			0.49	0.49	0.50	0.53	0.60
3743	232.4	114.6	1.857	0.000	0.543	0.216	0.907
	1		1.84	1.25	1.26	1.28	1.33
	2		1.32	1.15	1.15	1.06	0.30
			0.26	0.31	0.33	0.35	0.38
3744	473.5	128.8	4.671	0.000	1.367	0.440	1.020
	1		4.68	2.08	2.06	2.15	2.31
	2		2.31	2.24	2.28	2.21	0.59
			0.54	0.60	0.64	0.75	0.80
3745	345.7	140.2	4.912	0.000	1.438	0.321	1.110
	1		4.92	1.23	1.88	2.30	2.88
	2		2.87	2.69	2.66	2.53	0.49
			0.44	0.53	0.62	0.69	0.73
3746	180.7	141.4	3.061	0.000	0.896	0.168	1.120
	1		3.06	0.70	0.99	1.29	1.56
	2		1.55	1.32	1.33	1.25	0.29
			0.26	0.29	0.34	0.41	0.46
3747	76.1	142.4	1.406	0.000	0.411	0.071	1.127
	1		1.39	0.28	0.42	0.59	0.74
	2		0.73	0.61	0.60	0.58	0.18
			0.16	0.16	0.18	0.22	0.26
3748	638.0	127.2	5.714	0.000	1.672	0.593	1.007
	1		5.70	2.01	2.01	2.00	2.07
	2		19.75	2.31	2.32	2.27	0.70
			0.64	0.73	0.82	0.93	0.98
3749	465.6	128.0	4.488	0.000	1.313	0.433	1.013
	1		4.49	2.10	2.10	2.13	2.28

TABLE II. - Concluded.

XRUN	MASS FLOW G/S	TIN K	PIN MPA	PBACK MPA	PR	GR	TR
ORIFICE	INLET		POIN MPA	P1 MPA	P2 MPA	P3 MPA	POUT MPA
			PN1	PN2	PN3	PN4	PN5
3750	368.2	126.8	3.746	0.000	1.096	0.342	1.004
	1		3.75	1.73	1.85	1.92	2.08
				2.09			
	2		2.08	1.95	1.95	1.85	0.46
			0.41	0.48	0.53	0.59	0.64
3751	205.3	126.2	3.061	0.000	0.896	0.191	0.999
	1		3.02	0.82	1.31	1.45	1.81
				1.83			
	2		1.81	1.59	1.55	1.46	0.30
			0.27	0.32	0.37	0.42	0.46
3752	44.8	124.3	0.766	0.000	0.224	0.042	0.984
	1		0.71	0.15	0.22	0.29	0.36
				0.37			
	2		0.36	0.32	0.31	0.29	0.15
			0.13	0.13	0.14	0.16	0.21
3770	662.4	115.0	3.818	0.000	1.117	0.616	0.911
	1		3.75	0.55	0.54	0.54	0.54
				0.54			
	2		0.53	0.56	0.58	0.60	0.61
			0.60	0.60	0.61	0.68	0.80

XRUN	MASS FLOW G/S	TIN K	PIN MPA	PBACK MPA	PR	GR	TR
ORIFICE	INLET		POIN MPA	P1 MPA	P2 MPA	P3 MPA	POUT MPA
			PN1	PN2	PN3	PN4	PN5
3771	577.6	114.2	3.016	0.000	0.883	0.537	0.904
	1		2.95	0.51	0.50	0.50	0.50
				0.50			
	2		0.49	0.52	0.53	0.54	0.54
			0.53	0.53	0.54	0.59	0.69
3772	474.5	114.1	2.213	0.000	0.648	0.441	0.903
	1		2.15	0.47	0.46	0.47	0.46
				0.47			
	2		0.46	0.48	0.49	0.50	0.49
			0.48	0.48	0.48	0.52	0.59
3773	414.6	114.0	1.890	0.000	0.553	0.385	0.903
	1		1.82	0.50	0.49	0.50	0.49
				0.49			
	2		0.49	0.50	0.52	0.52	0.46
			0.45	0.46	0.47	0.51	0.57
3774	291.6	115.2	1.924	0.000	0.563	0.271	0.912
	1		1.89	1.18	1.18	1.20	1.22
				1.22			
	2		1.21	1.13	1.13	1.06	0.34
			0.37	0.37	0.38	0.40	0.44

TABLE III. - DATA FOR TWO SEQUENTIAL, AXIALLY ALINED ORIFICE INLETS - 0.66-DIAMETER SPACING WITH BACKPRESSURE

[Dimensions are in centimeters (inches).]

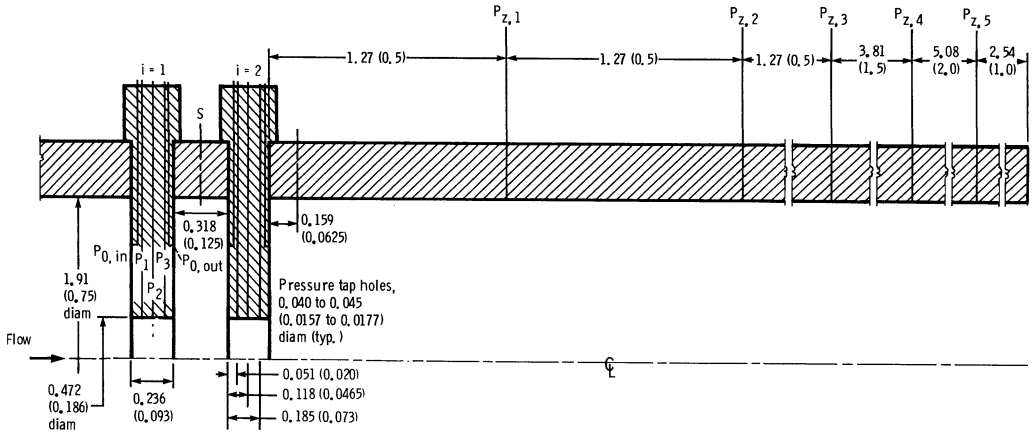

XRUN	MASS FLOW G/S	TIN K	PIN MPA	PBACK MPA	PR	GR	TR
ORIFICE INLET		POIN MPA	P1 MPA	P2 MPA	P3 MPA	POUT MPA	
		PN1	PN2	PN3	PN4	PN5	
3761	642.4	86.6	2.645	0.488	0.774	0.597	0.686
1		2.58	0.22	0.20	0.21	0.20	
		0.21					
2		0.20	0.21	0.22	0.24	0.28	
		0.27	0.27	0.28	0.28	0.49	
3762	638.3	87.1	2.641	0.577	0.773	0.593	0.690
1		2.58	0.23	0.22	0.22	0.22	
		0.22					
2		0.22	0.23	0.25	0.29	0.39	
		0.38	0.38	0.43	0.55	0.58	
3763	637.6	87.4	2.642	0.677	0.773	0.593	0.692
1		2.57	0.24	0.23	0.23	0.23	
		0.23					
2		0.23	0.25	0.27	0.34	0.49	
		0.48	0.49	0.56	0.64	0.68	
3764	626.3	90.1	2.655	0.849	0.777	0.582	0.713
1		2.59	0.30	0.29	0.29	0.28	
		0.28					
2		0.28	0.33	0.37	0.48	0.68	
		0.66	0.68	0.75	0.82	0.85	
3765	645.3	86.9	2.698	0.881	0.790	0.600	0.688
1		2.62	0.25	0.24	0.24	0.23	
		0.24					
2		0.23	0.28	0.32	0.47	0.71	
		0.69	0.71	0.78	0.85	0.88	
3766	641.3	87.4	2.702	1.099	0.791	0.596	0.692
1		2.63	0.26	0.25	0.26	0.25	
		0.26					
2		0.25	0.34	0.42	0.69	0.95	
		0.94	0.95	1.02	1.08	1.10	
3767	640.1	87.7	2.700	1.175	0.790	0.595	0.694
1		2.63	0.27	0.26	0.27	0.26	
		0.27					
2		0.26	0.38	0.48	0.77	1.03	
		1.01	1.02	1.09	1.15	1.18	
3768	614.8	88.4	2.747	1.334	0.804	0.571	0.700
1		2.71	0.52	0.54	0.64	0.72	
		0.74					
2		0.71	1.20	1.24	1.24	1.22	
		1.20	1.21	1.26	1.31	1.33	
3753	665.9	84.3	2.665	0.183	0.780	0.619	0.667
1		2.60	0.11	0.12	0.12	0.11	
		0.12					
2		0.11	0.12	0.12	0.13	0.13	
		0.11	0.12	0.11	0.12	0.18	
3754	664.0	84.4	0.661	0.177	0.194	0.617	0.668
1		0.52	0.00	0.10	0.10	0.00	
		0.10					
2		0.10	0.10	0.11	0.11	0.11	
		0.10	0.10	0.10	0.11	0.18	
3769	565.4	89.3	2.853	1.575	0.835	0.525	0.707
1		2.80	0.84	0.98	1.07	1.22	
		1.23					
2		1.20	1.47	1.51	1.51	1.46	
		1.45	1.46	1.51	1.55	1.58	

TABLE IV. - DATA FOR THREE SEQUENTIAL, AXIALLY ALINED ORIFICE INLETS - 0.66-DIAMETER SPACING

[Dimensions are in centimeters (inches).]

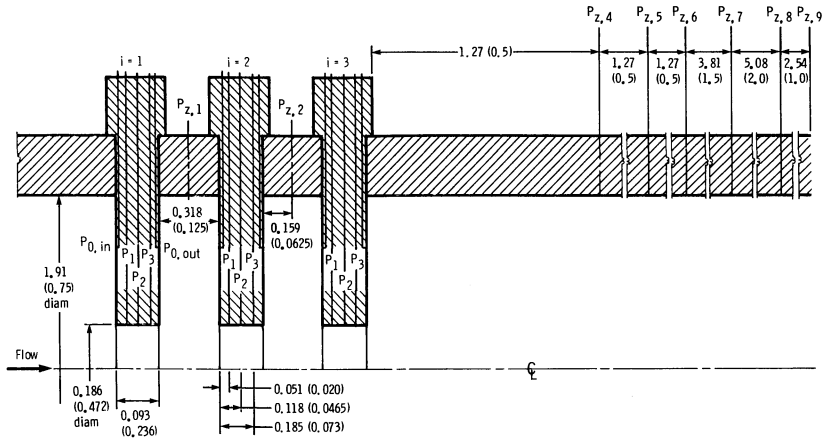

XRUN	MASS FLOW G/S	TIN K	PIN MPA	PBACK MPA	PR	GR	TR
ORIFICE INLET			POIN MPA	P1 MPA	P2 MPA	P3 MPA	POUT MPA
			PN1	PN2	PN3	PN4	PN5
3692	124.2	263.8	3.388	0.000	0.992	0.115	2.089
1			3.37	1.24	1.26	1.49	1.74
			1.76				
2			1.76	1.82	1.86	1.87	1.82
			1.83				
3			1.82	1.44	1.44	1.35	0.27
			0.27	0.29	0.34	0.42	0.39
3693	155.9	269.4	4.293	0.000	1.256	0.145	2.133
1			4.29	1.55	1.60	1.90	2.21
			2.23				
2			2.24	2.31	2.35	2.38	2.31
			2.32				
3			2.31	1.81	1.83	1.71	0.34
			0.33	0.36	0.42	0.53	0.50
3694	193.2	273.4	5.330	0.000	1.560	0.180	2.165
1			5.33	1.89	1.97	2.35	2.73
			2.77				
2			2.77	2.86	2.92	2.94	2.86
			2.88				
3			2.86	2.22	2.27	2.11	0.41
			0.41	0.44	0.51	0.65	0.63
3695	95.5	265.0	2.607	0.000	0.763	0.089	2.098
1			2.58	0.95	0.97	1.15	1.34
			1.35				
2			1.35	1.40	1.42	1.44	1.40
			1.40				
3			1.39	1.11	1.11	1.03	0.22
			0.22	0.24	0.27	0.33	0.30
3696	59.2	265.2	1.637	0.000	0.479	0.055	2.100
1			1.60	0.61	0.61	0.71	0.83
			0.85				
2			0.85	0.87	0.89	0.90	0.87
			0.88				
3			0.86	0.71	0.69	0.64	0.16
			0.16	0.17	0.19	0.23	0.30
3697	34.8	266.0	0.984	0.000	0.288	0.032	2.106
1			0.95	0.37	0.37	0.42	0.49
			0.50				
2			0.51	0.52	0.53	0.54	0.52
			0.52				
3			0.51	0.43	0.41	0.38	0.13
			0.14	0.14	0.15	0.17	0.14
3698	797.8	87.0	3.741	0.000	1.095	0.741	0.689
1			3.67	0.16	0.15	0.15	0.15
			0.16				
2			0.16	0.16	0.16	0.16	0.16
			0.16				
3			0.16	0.20	0.16	0.16	0.12
			0.12	0.13	0.13	0.16	0.23
3699	656.0	86.7	2.666	0.000	0.780	0.610	0.686
1			2.61	0.16	0.15	0.15	0.15
			0.16				
2			0.16	0.16	0.16	0.17	0.16
			0.16				
3			0.16	0.20	0.16	0.16	0.12
			0.13	0.12	0.13	0.14	0.14

XRUN	MASS FLOW G/S	TIN K	PIN MPA	PBACK MPA	PR	GR	TR
ORIFICE INLET			POIN MPA	P1 MPA	P2 MPA	P3 MPA	POUT MPA
			PN1	PN2	PN3	PN4	PN5
3700	544.4	86.3	1.897	0.000	0.555	0.506	0.683
1			1.85	0.16	0.15	0.15	0.15
			0.16				
2			0.16	0.16	0.16	0.16	0.16
			0.16				
3			0.15	0.19	0.15	0.15	0.13
			0.14	0.14	0.14	0.14	0.13
3701	386.2	86.8	0.060	0.000	0.018	0.359	0.687
1			0.35	0.18	0.17	0.17	0.17
			0.18				
2			0.18	0.17	0.17	0.18	0.17
			0.17				
3			0.17	0.22	0.17	0.18	0.17
			0.18	0.18	0.18	0.18	0.26
3702	642.4	117.7	4.112	0.000	1.203	0.597	0.932
1			4.07	0.95	0.93	0.93	0.93
			0.95				
2			0.95	1.13	1.17	1.24	1.35
			1.35				
3			1.35	1.40	1.38	1.31	0.60
			0.60	0.61	0.68	0.77	0.75
3703	513.3	127.5	4.750	0.000	1.390	0.477	1.010
1			4.74	2.19	2.18	2.19	2.30
			2.33				
2			2.33	2.22	2.27	2.32	2.46
			2.46				
3			2.36	2.32	2.22	0.58	0.60
			0.62	0.68	0.77	0.74	0.74
3704	287.8	127.0	3.433	0.000	1.005	0.267	1.006
1			3.43	1.66	1.76	1.86	1.95
			1.96				
2			1.97	1.94	1.95	1.96	1.95
			1.95				
3			1.94	1.78	1.73	1.63	0.37
			0.36	0.41	0.46	0.51	0.48
3705	188.5	126.9	2.973	0.000	0.870	0.175	1.005
1			2.96	1.20	1.33	1.58	1.76
			1.78				
2			1.78	1.77	1.79	1.80	1.78
			1.80				
3			1.77	1.51	1.47	1.38	0.26
			0.26	0.30	0.35	0.40	0.36
3706	103.4	128.0	1.815	0.000	0.531	0.096	1.013
1			1.78	0.67	0.69	0.83	0.95
			0.96				
2			0.96	0.99	1.00	1.01	0.98
			0.99				
3			0.98	0.81	0.78	0.73	0.18
			0.18	0.19	0.22	0.26	0.22
3707	77.0	127.6	1.366	0.000	0.400	0.072	1.010
1			1.31	0.50	0.51	0.60	0.72
			0.71				
2			0.71	0.73	0.74	0.74	0.75
			0.73				
3			0.73	0.60	0.57	0.54	0.19
			0.16	0.16	0.18	0.21	0.22

TABLE IV. - Concluded.

XRUN	MASS FLOW G/S	TIN K	PIN MPA	PBACK MPA	PR	GR	TR
3708	733.6	115.1	4.655	0.000	1.362	0.682	0.911
3709	596.2	114.3	3.462	0.000	1.013	0.554	0.905
3710	441.0	115.2	2.516	0.000	0.736	0.410	0.912
3711	244.5	114.9	1.889	0.000	0.553	0.227	0.910
3712	233.0	113.9	1.795	0.000	0.525	0.217	0.902

ORIFICE	INLET	POIN MPA	P1 MPA	P2 MPA	P3 MPA	POUT MPA
		PN1	PN2	PN3	PN4	PN5
3708	733.6	4.655	0.000	1.362	0.682	0.911
1		4.60	0.75	0.73	0.73	0.72
		0.73				
2		0.74	0.83	0.86	0.92	1.04
		1.04				
3		1.04	1.14	1.12	1.10	0.63
		0.62	0.62	0.66	0.73	0.80
3709	596.2	3.462	0.000	1.013	0.554	0.905
1		3.42	0.84	0.83	0.84	0.83
		0.84				
2		0.84	0.97	1.00	1.06	1.14
		1.15				
3		1.13	1.18	1.15	1.09	0.53
		0.53	0.54	0.58	0.63	0.72
3710	441.0	2.516	0.000	0.736	0.410	0.912
1		2.47	1.00	0.99	0.99	0.99
		1.00				
2		1.01	1.12	1.14	1.18	1.22
		1.22				
3		1.22	1.13	1.09	1.01	0.45
		0.45	0.50	0.55	0.56	0.66
3711	244.5	1.889	0.000	0.553	0.227	0.910
1		1.86	1.34	1.33	1.36	1.39
		1.40				
2		1.41	1.35	1.35	1.34	1.30
		1.31				
3		1.29	1.18	1.13	1.06	0.28
		0.27	0.32	0.35	0.35	0.31
3712	233.0	1.795	0.000	0.525	0.217	0.902
1		1.77	1.29	1.29	1.31	1.33
		1.34				
2		1.35	1.29	1.28	1.27	1.24
		1.24				
3		1.23	1.11	1.07	1.00	0.26
		0.26	0.30	0.33	0.34	0.30

XRUN	MASS FLOW G/S	TIN K	PIN MPA	PBACK MPA	PR	GR	TR
3713	421.4	140.1	5.553	0.000	1.625	0.392	1.109
3714	227.4	141.1	3.758	0.000	1.100	0.211	1.117
3715	101.3	141.6	1.915	0.000	0.560	0.094	1.121
3716	62.9	140.6	1.225	0.000	0.359	0.058	1.113

ORIFICE	INLET	POIN MPA	P1 MPA	P2 MPA	P3 MPA	POUT MPA
		PN1	PN2	PN3	PN4	PN5
3713	421.4	5.553	0.000	1.625	0.392	1.109
1		5.55	1.96	2.20	2.65	3.14
		3.17				
2		3.18	3.42	3.45	3.48	3.46
		3.47				
3		3.45	3.11	3.11	2.92	0.54
		0.52	0.63	0.72	0.79	0.78
3714	227.4	3.758	0.000	1.100	0.211	1.117
1		3.73	1.36	1.43	1.69	1.92
		1.94				
2		1.95	2.04	2.08	2.09	2.03
		2.05				
3		2.02	1.65	1.66	1.58	0.32
		0.31	0.37	0.43	0.49	0.45
3715	101.3	1.915	0.000	0.560	0.094	1.121
1		1.89	0.71	0.72	0.86	0.99
		1.01				
2		1.01	1.04	1.06	1.06	1.03
		1.04				
3		1.02	0.85	0.82	0.77	0.18
		0.18	0.20	0.22	0.27	0.24
3716	62.9	1.225	0.000	0.359	0.058	1.113
1		1.19	0.46	0.45	0.54	0.63
		0.64				
2		0.64	0.66	0.67	0.68	0.66
		0.65				
3		0.65	0.55	0.52	0.48	0.15
		0.15	0.15	0.17	0.20	0.17

TABLE V. - DATA FOR THREE SEQUENTIAL, AXIALLY ALINED ORIFICE INLETS - 0.66-DIAMETER SPACING WITH BACKPRESSURE

[Dimensions are in centimeters (inches).]

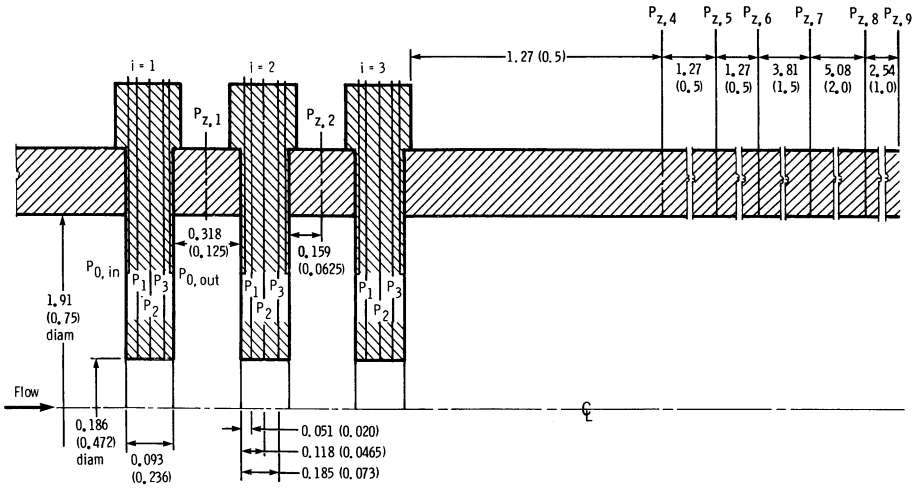

XRUN	MASS FLOW G/S	TIN K	PIN MPA	PBACK MPA	PR	GR	TR
ORIFICE INLET		POIN MPA	P1 MPA	P2 MPA	P3 MPA	POUT MPA	
		PN1	PN2	PN3	PN4	PN5	
3717	671.5	85.4	2.724	0.191	0.797	0.624	0.676
	1	2.66	0.15	0.14	0.14	0.14	
		0.15					
	2	0.15	0.15	0.15	0.15	0.16	
		0.15					
	3	0.15	0.19	0.16	0.16	0.16	
		0.17	0.17	0.17	0.17	0.19	
3718	666.3	85.8	2.723	0.428	0.797	0.619	0.679
	1	2.66	0.17	0.16	0.16	0.16	
		0.17					
	2	0.17	0.17	0.17	0.17	0.18	
		0.17					
	3	0.17	0.22	0.20	0.22	0.29	
		0.29	0.29	0.32	0.45	0.43	
3719	663.9	86.3	2.719	0.477	0.796	0.617	0.683
	1	2.66	0.18	0.17	0.17	0.17	
		0.18					
	2	0.18	0.17	0.18	0.18	0.18	
		0.17					
	3	0.17	0.23	0.21	0.23	0.29	
		0.29	0.29	0.32	0.44	0.48	
3720	659.9	87.1	2.722	0.563	0.797	0.613	0.690
	1	2.66	0.20	0.19	0.19	0.19	
		0.20					
	2	0.20	0.19	0.19	0.20	0.20	
		0.20					
	3	0.20	0.26	0.25	0.29	0.44	
		0.44	0.44	0.52	0.60	0.56	
3721	656.0	87.8	2.721	0.830	0.796	0.610	0.695
	1	2.66	0.22	0.21	0.20	0.20	
		0.21					
	2	0.21	0.21	0.21	0.22	0.22	
		0.22					
	3	0.22	0.31	0.31	0.44	0.72	
		0.72	0.73	0.82	0.87	0.83	
3722	644.1	90.3	2.728	1.086	0.798	0.599	0.715
	1	2.66	0.26	0.25	0.25	0.25	
		0.26					
	2	0.26	0.26	0.26	0.26	0.28	
		0.27					
	3	0.28	0.41	0.45	0.70	0.98	
		0.98	1.00	1.07	1.11	1.09	
3723	663.8	86.4	2.715	0.269	0.795	0.617	0.684
	1	2.64	0.17	0.16	0.16	0.16	
		0.17					
	2	0.17	0.17	0.17	0.17	0.17	
		0.17					
	3	0.17	0.22	0.19	0.20	0.22	
		0.22	0.22	0.22	0.26	0.27	
3724	651.4	86.8	2.729	1.265	0.799	0.605	0.687
	1	2.66	0.28	0.26	0.26	0.27	
		0.28					
	2	0.29	0.72	0.82	1.04	1.19	
		1.20					
	3	1.15	1.16	1.20	1.20	1.18	
		1.18	1.19	1.25	1.29	1.26	
3725	650.9	87.0	2.728	1.237	0.798	0.605	0.689
	1	2.66	0.28	0.26	0.26	0.26	
		0.27					
	2	0.27	0.50	0.58	0.82	1.09	
		1.13					
	3	1.09	1.15	1.18	1.18	1.16	
		1.16	1.17	1.22	1.26	1.24	
3726	577.7	87.9	2.888	1.561	0.845	0.537	0.696
	1	2.84	0.86	0.93	1.11	1.40	
		1.44					
	2	1.42	1.57	1.60	1.60	1.55	
		1.56					
	3	1.53	1.45	1.49	1.50	1.48	
		1.48	1.48	1.53	1.57	1.56	
3727	544.8	89.0	2.951	1.748	0.864	0.506	0.705
	1	2.91	1.16	1.12	1.25	1.56	
		1.62					
	2	1.62	1.75	1.79	1.78	1.74	
		1.76					
	3	1.72	1.66	1.71	1.71	1.69	
		1.69	1.71	1.75	1.78	1.75	
3728	445.0	91.1	3.138	2.320	0.918	0.414	0.721
	1	3.11	1.91	1.89	2.00	2.26	
		2.28					
	2	2.28	2.31	2.34	2.33	2.31	
		2.32					
	3	2.30	2.27	2.28	2.28	2.26	
		2.26	2.27	2.31	2.32	2.32	
3729	171.9	137.1	3.043	0.353	0.891	0.160	1.086
	1	3.02	1.12	1.16	1.37	1.56	
		1.59					
	2	1.59	1.65	1.69	1.69	1.65	
		1.66					
	3	1.64	1.33	1.33	1.25	0.25	
		0.26	0.29	0.34	0.39	0.35	

TABLE VI. - DATA FOR TWO SEQUENTIAL, AXIALLY ALINED ORIFICE INLETS - 32-DIAMETER SPACING

[Dimensions are in centimeters (inches).]

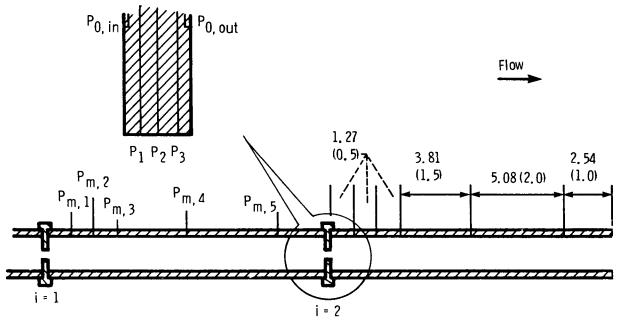

XRUN	MASS FLOW G/S	TIN K	PIN MPA	PBACK MPA	PR	GR	TR
ORIFICE INLET		POIN MPA	P1 MPA	P2 MPA	P3 MPA	POUT MPA	
			PM1	PM2	PM3	PM4	PM5
3254	32.9	254.0	1.140	0.000	0.334	0.031	2.011
	1		1.11	0.76	0.74	0.80	0.85
			0.86	0.86	0.86	0.87	
	2		0.87	0.18	0.28	0.35	0.15
			0.14	0.14	0.18	0.19	0.19
3255	49.8	251.0	1.692	0.000	0.495	0.046	1.987
	1		1.67	1.13	1.12	1.20	1.28
			1.28	1.28	1.30	1.31	
	2		1.31	0.26	0.40	0.51	0.17
			0.16	0.16	0.19	0.22	0.24
3256	73.3	252.0	2.466	0.000	0.722	0.068	1.995
	1		2.46	1.64	1.64	1.75	1.88
			1.88	1.88	1.90	1.92	
	2		1.92	0.38	0.57	0.75	0.20
			0.20	0.19	0.23	0.29	0.30
3257	132.3	257.0	4.446	0.000	1.301	0.123	2.035
	1		4.47	2.95	2.98	3.16	3.41
			3.41	3.42	3.45	3.50	
	2		3.49	0.64	1.01	1.36	0.31
			0.31	0.30	0.35	0.48	0.50
3258	181.0	263.9	6.118	0.000	1.790	0.168	2.089
	1		6.18	4.04	4.08	4.36	4.72
			4.71	4.73	4.77	4.83	
	2		4.82	0.84	1.38	1.89	0.41
			0.40	0.40	0.48	0.63	0.66
3259	757.0	84.3	5.628	0.000	1.647	0.704	0.667
	1		5.62	2.26	2.34	2.68	3.23
			3.23	3.26	3.35	3.41	
	2		3.41	0.18	0.16	0.16	0.18
			0.16	0.14	0.35	0.19	0.30
3260	656.0	84.8	4.335	0.000	1.269	0.610	0.671
	1		4.32	1.80	1.83	2.02	2.46
			2.46	2.49	2.56	2.60	
	2		2.60	0.15	0.13	0.14	0.14
			0.13	0.12	0.19	0.14	0.20
3261	545.0	85.3	3.190	0.000	0.934	0.507	0.675
	1		3.17	1.46	1.44	1.52	1.74
			1.74	1.76	1.82	1.86	
	2		1.86	0.16	0.14	0.15	0.15
			0.14	0.13	0.16	0.16	0.20
3262	440.0	84.4	2.058	0.000	0.602	0.409	0.668
	1		2.02	0.88	0.88	0.97	1.21
			1.21	1.22	1.26	1.26	
	2		1.26	0.16	0.15	0.15	0.16
			0.15	0.14	0.18	0.16	0.19
3263	366.0	84.8	1.574	0.000	0.461	0.340	0.671
	1		1.53	0.76	0.74	0.78	0.91
			0.91	0.91	0.95	0.95	
	2		0.96	0.19	0.18	0.18	0.19
			0.18	0.17	0.20	0.20	0.22
3264	306.6	85.4	1.213	0.000	0.355	0.285	0.676
	1		1.18	0.63	0.61	0.64	0.71
			0.71	0.72	0.73	0.75	
	2		0.75	0.20	0.19	0.19	0.19
			0.19	0.18	0.21	0.20	0.22
3265	306.6	85.9	1.208	0.000	0.354	0.285	0.680
	1		1.18	0.64	0.61	0.64	0.71
			0.71	0.71	0.73	0.75	
	2		0.75	0.21	0.19	0.19	0.20
			0.19	0.18	0.21	0.20	0.22
3266	639.7	114.4	5.742	0.000	1.680	0.595	0.906
	1		5.75	2.78	2.80	2.99	3.42
			3.41	3.46	3.53	3.60	
	2		3.58	0.61	0.60	0.60	0.61
			0.60	0.58	0.62	0.70	0.77
3267	548.6	114.1	4.381	0.000	1.282	0.510	0.903
	1		4.38	2.13	2.16	2.31	2.64
			2.64	2.66	2.73	2.77	
	2		2.76	0.55	0.53	0.54	0.54
			0.55	0.52	0.55	0.62	0.66
3268	447.8	113.4	3.220	0.000	0.942	0.416	0.898
	1		3.20	1.74	1.72	1.75	1.87
			1.87	1.89	1.93	1.97	
	2		1.97	0.49	0.48	0.48	0.48
			0.49	0.47	0.49	0.53	0.56
3269	323.2	113.4	2.390	0.000	0.699	0.300	0.898
	1		2.38	1.61	1.60	1.60	1.64
			1.64	1.64	1.66	1.70	
	2		1.70	0.81	0.81	0.83	0.38
			0.40	0.41	0.43	0.44	0.44
3270	371.0	141.0	6.035	0.000	1.766	0.345	1.116
	1		6.09	4.08	4.09	4.37	4.74
			4.73	4.75	4.79	4.84	
	2		4.82	1.76	2.01	2.41	0.48
			0.47	0.53	0.61	0.72	0.73
3271	232.9	140.9	4.486	0.000	1.313	0.216	1.116
	1		4.51	3.05	3.05	3.24	3.50
			3.49	3.51	3.53	3.58	
	2		3.57	1.02	1.41	1.73	0.33
			0.32	0.35	0.41	0.50	0.51
3272	140.6	141.4	3.083	0.000	0.902	0.131	1.120
	1		3.08	2.06	2.06	2.18	2.35
			2.35	2.35	2.38	2.40	
	2		2.40	0.47	0.77	0.98	0.24
			0.23	0.24	0.29	0.36	0.36
3273	92.8	141.8	2.144	0.000	0.627	0.086	1.123
	1		2.13	1.43	1.42	1.52	1.63
			1.63	1.63	1.65	1.66	
	2		1.66	0.32	0.51	0.67	0.19
			0.18	0.18	0.22	0.26	0.28

TABLE VI. - Concluded.

XRUN	MASS FLOW G/S	TIN K	PIN MPA	PBACK MPA	PR	GR	TR
3274	35.4	142.6	0.897	0.000	0.263	0.033	1.129
3275	509.0	126.8	5.875	0.000	1.719	0.473	1.004
3276	398.0	126.9	4.697	0.000	1.375	0.370	1.005
3277	248.7	127.5	3.614	0.000	1.058	0.231	1.010
3278	183.2	126.2	3.299	0.000	0.965	0.170	0.999
3279	186.8	126.8	3.392	0.000	0.993	0.174	1.004
3280	84.4	127.1	1.807	0.000	0.529	0.078	1.006

XRUN	ORIFICE	INLET	POIN MPA	P1 MPA	P2 MPA	P3 MPA	POUT MPA
			PM1	PM2	PM3	PM4	PM5
3274	1		0.87	0.61	0.59	0.63	0.66
			0.67	0.67	0.68	0.68	
	2		0.68	0.15	0.21	0.27	0.15
			0.14	0.13	0.16	0.18	0.18
3275	1		5.91	3.67	3.69	3.79	4.09
			4.08	4.11	4.18	4.22	
	2		4.22	1.67	1.69	1.77	0.75
			0.72	0.75	0.82	0.91	0.93
3276	1		4.72	3.26	3.27	3.35	3.57
			3.56	3.60	3.63	3.65	
	2		3.65	1.82	1.86	1.94	0.48
			0.47	0.52	0.58	0.64	0.65
3277	1		3.63	2.80	2.79	2.81	2.86
			2.86	2.87	2.89	2.92	
	2		2.92	1.28	1.41	1.41	0.34
			0.33	0.34	0.40	0.46	0.48
3278	1		3.30	2.49	2.48	2.50	2.54
			2.54	2.54	2.55	2.60	
	2		2.60	1.02	1.15	1.17	0.28
			0.27	0.28	0.33	0.40	0.42
3279	1		3.40	2.55	2.55	2.56	2.62
			2.62	2.62	2.64	2.67	
	2		2.67	1.04	1.18	1.20	0.29
			0.28	0.29	0.34	0.41	0.42
3280	1		1.78	1.21	1.20	1.28	1.36
			1.37	1.37	1.38	1.40	
	2		1.40	0.29	0.44	0.56	0.18
			0.18	0.17	0.25	0.24	0.25

TABLE VII. - DATA FOR TWO SEQUENTIAL, AXIALLY ALINED ORIFICE INLETS - 32-DIAMETER SPACING WITH BACKPRESSURE

[Dimensions are in centimeters (inches).]

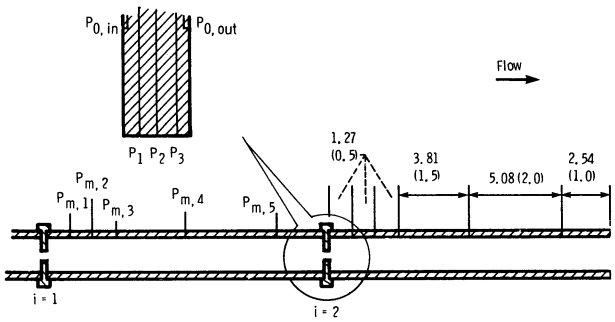

XRUN	MASS FLOW G/S	TIN K	PIN MPA	PBACK MPA	PR	GR	TR
3281	30.0	272.0	1.075	0.185	0.315	0.028	2.154
3282	110.0	271.3	3.812	0.851	1.116	0.102	2.148
3283	111.0	269.0	3.819	1.023	1.118	0.103	2.130
3284	110.5	268.0	3.820	1.106	1.118	0.103	2.122
3285	111.0	267.5	3.820	1.154	1.118	0.103	2.118
3286	614.0	86.9	3.851	0.160	1.127	0.571	0.688
3287	603.0	87.4	3.862	0.303	1.130	0.560	0.692
3288	600.0	88.0	3.865	0.428	1.131	0.558	0.697
3289	586.0	88.8	3.896	0.789	1.140	0.545	0.703
3290	582.0	89.2	3.903	1.044	1.142	0.541	0.706

ORIFICE INLET		POIN MPA	P1 MPA	P2 MPA	P3 MPA	POUT MPA
			PM1	PM2	PM3	PM4	PM5
3281	30.0	272.0	1.075	0.185	0.315	0.028	2.154
	1		1.04	0.71	0.69	0.74	0.80
			0.81	0.80	0.82	0.82	
	2		0.82	0.17	0.27	0.33	0.15
			0.14	0.13	0.35	0.18	0.19
3282	110.0	271.3	3.812	0.851	1.116	0.102	2.148
	1		3.82	2.53	2.53	2.70	2.92
			2.92	2.92	2.95	2.98	
	2		2.98	0.55	0.88	1.15	0.71
			0.71	0.69	0.74	0.85	0.86
3283	111.0	269.0	3.819	1.023	1.118	0.103	2.130
	1		3.83	2.54	2.54	2.71	2.92
			2.93	2.93	2.96	3.00	
	2		3.00	0.55	0.89	1.16	0.89
			0.89	0.86	0.93	1.02	1.03
3284	110.5	268.0	3.820	1.106	1.118	0.103	2.122
	1		3.83	2.54	2.54	2.71	2.93
			2.93	2.93	2.96	2.99	
	2		2.99	0.55	0.89	1.16	0.98
			0.98	0.96	1.04	1.11	1.11
3285	111.0	267.5	3.820	1.154	1.118	0.103	2.118
	1		3.83	2.54	2.53	2.71	2.93
			2.93	2.93	2.96	3.00	
	2		2.99	0.55	0.89	1.16	1.03
			1.02	1.01	1.09	1.15	1.16
3286	614.0	86.9	3.851	0.160	1.127	0.571	0.688
	1		3.84	1.65	1.67	1.84	2.19
			2.19	2.21	2.29	2.32	
	2		2.32	0.16	0.15	0.14	0.15
			0.15	0.14	0.18	0.16	0.20
3287	603.0	87.4	3.862	0.303	1.130	0.560	0.692
	1		3.84	1.71	1.73	1.91	2.24
			2.24	2.25	2.32	2.35	
	2		2.36	0.26	0.24	0.23	0.25
			0.25	0.24	0.27	0.30	0.41
3288	600.0	88.0	3.865	0.428	1.131	0.558	0.697
	1		3.85	1.73	1.75	1.90	2.26
			2.26	2.29	2.35	2.38	
	2		2.40	0.31	0.29	0.28	0.31
			0.32	0.30	0.34	0.43	0.47
3289	586.0	88.8	3.896	0.789	1.140	0.545	0.703
	1		3.89	1.84	1.86	2.02	2.35
			2.35	2.38	2.44	2.47	
	2		2.47	0.46	0.43	0.47	0.65
			0.65	0.65	0.74	0.79	0.79
3290	582.0	89.2	3.903	1.044	1.142	0.541	0.706
	1		3.89	1.85	1.86	2.02	2.46
			2.46	2.49	2.54	2.57	
	2		2.58	0.55	0.55	0.66	0.93
			0.93	0.93	1.01	1.04	1.05

XRUN	MASS FLOW G/S	TIN K	PIN MPA	PBACK MPA	PR	GR	TR
3291	574.0	89.9	3.915	1.154	1.146	0.533	0.712
3293	487.0	92.3	4.078	2.134	1.193	0.453	0.731
3294	508.0	115.1	3.988	0.608	1.167	0.472	0.911
3295	491.0	115.6	4.018	0.961	1.176	0.456	0.915
3296	512.0	114.4	3.975	0.589	1.163	0.476	0.906
3297	493.0	114.7	4.010	0.968	1.174	0.458	0.908
3298	474.0	115.3	4.040	1.272	1.182	0.441	0.913
3299	442.0	116.2	4.094	1.761	1.198	0.411	0.920
3301	130.0	225.0	4.082	0.442	1.195	0.121	1.781
3302	131.0	222.0	4.076	0.699	1.193	0.122	1.758

ORIFICE INLET		POIN MPA	P1 MPA	P2 MPA	P3 MPA	POUT MPA
			PM1	PM2	PM3	PM4	PM5
3291	574.0	89.9	3.915	1.154	1.146	0.533	0.712
	1		3.90	1.89	1.91	2.08	2.53
			2.53	2.55	2.61	2.64	
	2		2.64	0.65	0.68	0.78	1.05
			1.05	1.05	1.15	1.15	1.16
3293	487.0	92.3	4.078	2.134	1.193	0.453	0.731
	1		4.08	2.52	2.60	2.95	3.12
			3.13	3.14	3.18	3.20	
	2		3.20	1.77	1.71	1.78	2.06
			2.05	2.06	2.17	2.14	2.15
3294	508.0	115.1	3.988	0.608	1.167	0.472	0.911
	1		3.98	2.04	2.04	2.11	2.38
			2.38	2.40	2.46	2.49	
	2		2.50	0.56	0.54	0.54	0.54
			0.55	0.56	0.56	0.61	0.65
3295	491.0	115.6	4.018	0.961	1.176	0.456	0.915
	1		4.02	2.18	2.20	2.30	2.58
			2.58	2.60	2.64	2.68	
	2		2.69	0.88	0.86	0.85	0.88
			0.89	0.86	0.90	0.97	1.00
3296	512.0	114.4	3.975	0.589	1.163	0.476	0.906
	1		3.97	2.01	2.01	2.10	2.36
			2.37	2.39	2.44	2.48	
	2		2.49	0.54	0.53	0.52	0.53
			0.53	0.51	0.54	0.11	0.64
3297	493.0	114.7	4.010	0.968	1.174	0.458	0.908
	1		4.00	2.18	2.19	2.30	2.57
			2.57	2.59	2.64	2.68	
	2		2.69	0.88	0.86	0.85	0.89
			0.89	0.87	0.94	0.98	1.01
3298	474.0	115.3	4.040	1.272	1.182	0.441	0.913
	1		4.03	2.33	2.35	2.47	2.73
			2.73	2.75	2.80	27.41	
	2		2.83	1.16	1.13	1.13	1.18
			1.18	1.16	1.20	1.27	1.29
3299	442.0	116.2	4.094	1.761	1.198	0.411	0.920
	1		4.10	2.60	2.62	2.73	2.96
			2.96	2.98	3.02	3.04	
	2		3.04	1.58	1.55	1.55	1.67
			1.66	1.66	1.71	1.76	1.77
3301	130.0	225.0	4.082	0.442	1.195	0.121	1.781
	1		4.10	2.71	2.71	2.89	3.12
			3.12	3.13	3.16	3.20	
	2		3.20	0.58	0.94	1.25	0.29
			0.30	0.28	0.34	0.44	0.47
3302	131.0	222.0	4.076	0.699	1.193	0.122	1.758
	1		4.09	2.71	2.70	2.89	3.12
			3.12	3.13	3.16	3.19	
	2		3.19	0.58	0.94	1.24	0.54
			0.55	0.52	0.57	0.70	0.71

TABLE VII. - Concluded.

XRUN	MASS FLOW G/S	TIN K	PIN MPA	PBACK MPA	PR	GR	TR
3303	131.0	224.0	4.066	0.920	1.190	0.122	1.774
3304	129.8	226.0	4.061	1.313	1.188	0.121	1.789
3305	129.2	229.0	4.063	1.727	1.189	0.120	1.813
3306	122.1	231.0	4.108	2.044	1.202	0.113	1.829
3307	119.4	233.0	4.131	2.327	1.209	0.111	1.845
3308	114.3	234.0	4.168	2.617	1.220	0.106	1.853
3000	0.0	0.0	0.000	3.686	0.000	0.000	0.000

ORIFICE	INLET	POIN MPA	P1 MPA	P2 MPA	P3 MPA	POUT MPA
		PM1	PM2	PM3	PM4	PM5
1		4.09	2.70	2.69	2.89	3.11
		3.11	3.12	3.15	3.19	
2		3.19	0.58	0.94	1.24	0.77
		0.77	0.75	0.80	0.92	0.93
1		4.08	2.70	2.69	2.88	3.11
		3.11	3.12	3.15	3.18	
2		3.18	0.58	0.94	1.24	1.19
		1.18	1.16	1.35	1.31	1.32
1		4.08	2.71	2.69	2.88	3.11
		3.11	3.12	3.15	3.18	
2		3.18	0.58	0.93	1.26	1.63
		1.62	1.61	1.68	1.73	1.73
1		4.13	2.91	2.91	3.07	3.29
		3.29	3.29	3.32	3.35	
2		3.35	1.66	1.62	1.72	1.96
		1.94	1.93	2.02	2.04	2.04
1		4.15	3.00	3.00	3.13	3.33
		3.33	3.34	3.37	3.40	
2		3.40	1.82	1.79	1.97	2.27
		2.25	2.25	2.32	2.33	2.33
1		4.19	3.15	3.15	3.26	3.44
		3.44	3.44	3.47	3.50	
2		3.49	2.15	2.13	2.35	2.57
		2.55	2.55	2.62	2.62	2.62
1		0.00	0.00	0.00	0.00	0.00
		0.00	0.00	0.00	0.00	
2		0.00	0.00	0.00	22.92	0.81
		3.49	3.64	3.64	3.64	3.66

TABLE VIII. - DATA FOR THREE SEQUENTIAL, AXIALLY ALINED ORIFICE INLETS - 32-DIAMETER SPACING
[Dimensions are in centimeters (inches).]

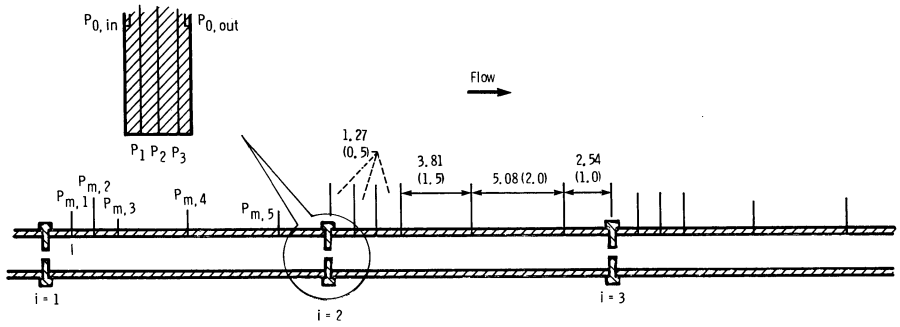

XRUN	MASS FLOW G/S	TIN K	PIN MPA	PBACK MPA	PR	GR	TR
3217	35.0	262.0	1.439	0.000	0.421	0.033	2.074
3218	49.7	263.0	2.028	0.000	0.594	0.046	2.082
3219	90.5	267.0	3.695	0.000	1.081	0.084	2.114
3220	90.8	266.0	3.695	0.000	1.081	0.084	2.106
3221	117.0	272.0	4.776	0.000	1.398	0.109	2.154
3222	117.2	268.5	4.779	0.000	1.399	0.109	2.126
3223	570.0	88.5	4.737	0.000	1.386	0.530	0.701
3224	473.0	89.0	3.236	0.000	0.947	0.440	0.705
3225	434.0	88.9	2.808	0.000	0.822	0.403	0.704

ORIFICE INLET	POIN MPA	P1 MPA	P2 MPA	P3 MPA	POUT MPA
		PM1	PM2	PM3	PM4
3217	1.439	0.000	0.421	0.033	2.074
1		1.41	1.11	1.09	1.13	1.18
		1.19	1.18	1.18	1.20	
2		1.20	0.78	0.78	0.84	0.92
3		0.94	0.17	0.25	0.35	0.14
		0.15	0.14	0.18	0.19	0.20
3218	2.028	0.000	0.594	0.046	2.082
1		2.01	1.57	1.55	1.60	1.69
		1.67	1.68	1.69	1.70	
2		1.71	1.12	1.11	1.21	1.31
3		1.34	0.25	0.35	0.49	0.16
		0.17	0.16	0.19	0.23	0.24
3219	3.695	0.000	1.081	0.084	2.114
1		3.71	2.85	2.86	2.95	3.09
		3.09	3.10	3.11	3.14	
2		3.14	2.06	2.04	2.23	2.41
3		2.46	0.45	0.61	0.89	0.22
		0.23	0.23	0.27	0.35	0.37
3220	3.695	0.000	1.081	0.084	2.106
1		3.71	2.86	2.86	2.96	3.10
		3.09	3.10	3.12	3.15	
2		3.14	2.06	2.06	2.23	2.41
3		2.46	0.45	0.60	0.90	0.58
		0.59	0.57	0.62	0.70	0.71
3221	4.776	0.000	1.398	0.109	2.154
1		4.81	3.68	3.71	3.82	4.01
		4.00	4.02	4.04	4.07	
2		4.06	2.66	2.66	2.89	3.11
3		3.18	0.57	0.76	1.16	0.71
		0.73	0.71	0.76	0.88	0.89
3222	4.779	0.000	1.399	0.109	2.126
1		4.82	3.69	3.71	3.82	4.01
		4.00	4.02	4.04	4.07	
2		4.06	2.66	2.66	2.89	3.11
3		3.18	0.57	0.76	1.16	0.27
		0.29	0.28	0.33	0.43	0.46
3223	4.737	0.000	1.386	0.530	0.701
1		4.74	2.72	2.74	3.23	3.41
		3.40	3.44	3.47	3.51	
2		3.50	1.59	1.56	1.70	2.07
3		2.18	0.31	0.28	0.28	0.30
		0.31	0.29	0.32	0.38	0.44
3224	3.236	0.000	0.947	0.440	0.705
1		3.23	1.84	1.84	2.18	2.35
		2.35	2.38	2.40	2.42	
2		2.42	1.10	1.08	1.17	1.43
3		1.50	0.22	0.20	0.20	0.20
		0.21	0.20	0.22	0.23	0.27
3225	2.808	0.000	0.822	0.403	0.704
1		2.79	1.65	1.63	1.85	2.06
		2.06	2.07	2.10	2.12	
2		2.11	1.01	0.98	1.04	1.24
3		1.31	0.22	0.21	0.21	0.21
		0.22	0.21	0.33	0.24	0.26

XRUN	MASS FLOW G/S	TIN K	PIN MPA	PBACK MPA	PR	GR	TR
3226	369.0	88.7	2.107	0.000	0.617	0.343	0.702
3227	307.0	89.1	1.626	0.000	0.476	0.285	0.705
3228	273.0	89.3	1.335	0.000	0.391	0.254	0.707
3229	642.0	91.8	5.775	0.000	1.690	0.597	0.727
3230	643.0	85.7	5.680	0.000	1.662	0.598	0.679
3231	633.0	85.7	5.669	0.000	1.659	0.588	0.679
3232	623.5	86.1	5.670	0.000	1.659	0.579	0.682
3233	616.8	86.6	5.675	0.000	1.661	0.573	0.686
3234	600.5	86.9	5.708	0.000	1.670	0.558	0.688

ORIFICE INLET	POIN MPA	P1 MPA	P2 MPA	P3 MPA	POUT MPA
		PM1	PM2	PM3	PM4
3226	2.107	0.000	0.617	0.343	0.702
1		2.08	1.26	1.24	1.34	1.53
		1.52	1.54	1.55	1.57	
2		1.57	0.75	0.72	0.78	0.97
3		1.02	0.22	0.21	0.21	0.21
		0.22	0.21	0.23	0.24	0.25
3227	1.626	0.000	0.476	0.285	0.705
1		1.60	1.05	1.02	1.06	1.16
		1.16	1.17	1.18	1.20	
2		1.20	0.63	0.62	0.65	0.74
3		0.77	0.22	0.21	0.21	0.21
		0.22	0.21	0.23	0.23	0.24
3228	1.335	0.000	0.391	0.254	0.707
1		1.30	0.85	0.84	0.88	0.95
		0.95	0.96	0.98	0.99	
2		0.98	0.53	0.52	0.54	0.64
3		0.66	0.22	0.21	0.21	0.21
		0.22	0.21	0.23	0.23	0.24
3229	5.775	0.000	1.690	0.597	0.727
1		5.80	3.15	3.24	3.58	4.20
		4.18	4.22	4.27	4.32	
2		4.31	1.78	1.75	2.01	2.56
3		2.70	0.24	0.22	0.22	0.23
		0.24	0.22	0.25	0.27	0.33
3230	5.680	0.000	1.662	0.598	0.679
1		5.70	3.22	3.25	3.57	3.99
		3.98	3.98	4.09	4.13	
2		4.12	1.84	1.78	1.95	2.42
3		2.55	0.32	0.30	0.31	0.37
		0.38	0.38	0.58	0.53	0.54
3231	5.669	0.000	1.659	0.588	0.679
1		5.69	3.31	3.32	3.63	4.04
		4.04	4.08	4.14	4.18	
2		4.18	1.91	1.84	2.00	2.47
3		2.60	0.37	0.33	0.36	0.48
		0.48	0.48	0.58	0.64	0.65
3232	5.670	0.000	1.659	0.579	0.682
1		5.69	3.35	3.38	3.69	4.09
		4.08	4.11	4.18	4.22	
2		4.21	1.98	1.91	2.06	2.54
3		2.66	0.44	0.41	0.51	0.70
		0.71	0.72	0.81	0.86	0.86
3233	5.675	0.000	1.661	0.573	0.686
1		5.71	3.30	3.38	4.04	4.21
		4.20	4.24	4.28	4.32	
2		4.31	2.12	2.04	2.22	2.65
3		2.78	0.56	0.55	0.74	0.97
		1.00	1.00	1.08	1.12	1.11
3234	5.708	0.000	1.670	0.558	0.688
1		5.73	3.47	3.53	4.08	4.31
		4.30	4.34	4.38	4.42	
2		4.40	2.31	2.24	2.43	2.85
3		2.97	0.86	0.84	1.07	1.40
		1.40	1.40	1.48	1.51	1.51

TABLE VIII. - Concluded.

XRUN	MASS FLOW G/S	TIN K	PIN MPA	PBACK MPA	PR	GR	TR
3235	511.1	88.3	5.883	0.000	1.722	0.475	0.699
3236	491.0	88.2	3.478	0.000	1.018	0.456	0.698
3237	563.0	113.5	5.800	0.000	1.697	0.523	0.899
3238	462.7	113.2	4.245	0.000	1.242	0.430	0.896
3239	346.7	114.0	3.071	0.000	0.899	0.322	0.903
3240	340.6	114.6	3.074	0.000	0.900	0.317	0.907
3241	338.0	114.8	3.075	0.000	0.900	0.314	0.909
3242	329.0	115.1	3.082	0.000	0.902	0.306	0.911
3243	240.0	114.2	2.323	0.000	0.680	0.223	0.904
3244	197.5	113.7	1.971	0.000	0.577	0.184	0.900

ORIFICE INLET	POIN MPA	P1 MPA	P2 MPA	P3 MPA	POUT MPA
		PM1	PM2	PM3	PM4
1	5.93	4.31	4.38	4.71	4.95
		4.94	4.98	5.00	5.04
2	5.01	3.46	3.42	3.55	3.92
3	4.00	2.48	2.37	2.46	2.80
		2.80	2.81	2.91	2.88	2.89
1	3.46	1.97	2.00	2.35	2.55
		2.55	2.55	2.58	2.61
2	2.61	1.18	1.14	1.24	1.51
3	1.60	0.21	0.19	0.19	0.19
		0.20	0.19	0.21	0.22	0.26
1	5.83	3.47	3.55	3.93	4.28
		4.27	4.31	4.35	4.40
2	4.39	2.11	2.18	2.37	2.72
3	2.85	0.61	0.58	0.58	0.58
		0.59	0.57	0.60	0.67	0.72
1	4.25	2.68	2.70	2.89	3.14
		3.13	3.17	3.20	3.22
2	3.22	1.69	15.75	1.71	1.95
3	2.04	0.50	0.48	0.48	0.48
		0.50	0.48	0.55	0.54	0.58
1	3.06	2.15	2.16	2.26	2.43
		2.43	2.45	2.46	2.48
2	2.47	1.59	1.57	1.59	1.69
3	1.74	0.76	0.76	0.80	0.38
		0.42	0.44	0.46	0.47	0.47
1	3.07	2.20	2.20	2.29	2.44
		2.44	2.46	2.48	2.50
2	2.49	1.64	1.62	1.63	1.72
3	1.78	0.84	0.82	0.84	0.84
		0.85	0.84	0.86	0.90	0.91
1	3.07	2.22	2.21	2.31	2.46
		2.46	2.47	2.49	2.50
2	2.50	1.65	1.63	1.64	1.75
3	1.81	0.91	0.89	0.91	0.93
		0.95	0.93	0.96	1.00	1.01
1	3.08	2.26	2.26	2.35	2.49
		2.49	2.51	2.53	2.53
2	2.53	1.73	1.71	1.72	1.82
3	1.87	1.07	1.04	1.05	1.06
		1.08	1.06	1.09	1.12	1.13
1	2.31	1.89	1.88	1.92	1.97
		1.97	1.98	1.98	1.99
2	1.99	1.57	1.56	1.56	1.60
3	1.63	0.99	0.98	1.00	0.28
		0.30	0.32	0.34	0.36	0.36
1	1.95	1.68	1.67	1.68	1.69
		1.69	1.69	1.69	1.71
2	1.71	1.37	1.36	1.38	1.42
3	1.44	0.87	0.87	0.86	0.24
		0.25	0.26	0.30	0.31	0.32

XRUN	MASS FLOW G/S	TIN K	PIN MPA	PBACK MPA	PR	GR	TR
3245	317.8	140.8	6.038	0.000	1.767	0.295	1.115
3246	153.0	142.4	3.758	0.000	1.100	0.142	1.127
3247	70.0	126.2	1.756	0.000	0.514	0.065	0.999
3248	85.0	142.9	2.292	0.000	0.671	0.079	1.131
3249	60.0	142.2	1.666	0.000	0.488	0.056	1.126
3250	304.4	127.0	4.329	0.000	1.267	0.283	1.006
3251	202.0	126.9	3.462	0.000	1.013	0.188	1.005
3252	113.4	126.0	2.644	0.000	0.774	0.105	0.998
3253	55.2	128.8	1.463	0.000	0.428	0.051	1.020

ORIFICE INLET	POIN MPA	P1 MPA	P2 MPA	P3 MPA	POUT MPA
		PN1	PN2	PN3	PN4	PN5
1	6.09	4.65	4.64	4.87	5.13
		5.12	5.15	5.17	5.21
2	5.20	3.61	3.58	3.83	4.15
3	4.24	1.53	1.68	2.08	0.41
		0.41	0.44	0.52	0.62	0.64
1	3.78	2.91	2.91	3.00	3.14
		3.14	3.15	3.17	3.19
2	3.19	2.09	2.09	2.30	2.46
3	2.51	0.51	0.70	1.02	0.24
		0.24	0.25	0.31	0.37	0.38
1	1.73	1.35	1.34	1.39	1.44
		1.44	1.44	1.46	1.46
2	1.46	0.97	0.97	1.05	1.13
3	1.15	0.23	0.29	0.44	0.16
		0.16	0.16	0.20	0.22	0.23
1	2.26	1.76	1.75	1.81	1.89
		1.89	1.90	1.91	1.93
2	1.93	1.27	1.26	1.37	1.49
3	1.52	0.28	0.37	0.58	0.17
		0.18	0.17	0.21	0.25	0.26
1	1.64	1.29	1.28	1.32	1.37
		1.38	1.38	1.38	1.40
2	1.40	0.92	0.91	1.00	1.07
3	1.10	0.21	0.27	0.41	0.15
		0.16	0.15	0.19	0.21	0.22
1	4.35	3.47	3.48	3.55	3.69
		3.68	3.70	3.71	3.74
2	3.73	2.86	2.85	2.88	2.98
3	3.04	1.42	1.46	1.49	0.37
		0.37	0.39	0.45	0.50	0.52
1	3.48	2.93	2.93	2.95	2.99
		2.99	2.99	3.00	3.02
2	3.02	2.30	2.29	2.31	2.37
3	2.42	1.09	1.12	1.09	0.27
		0.28	0.28	0.43	0.38	0.41
1	2.65	2.09	2.08	2.15	2.22
		2.23	2.24	2.25	2.26
2	2.26	1.53	1.52	1.64	1.77
3	1.80	0.53	0.62	0.84	0.18
		0.19	0.19	0.26	0.28	0.29
1	1.44	1.13	1.12	1.15	1.20
		1.20	1.20	1.21	1.22
2	1.22	0.80	0.80	0.87	0.94
3	0.96	0.19	0.24	0.36	0.15
		0.15	0.14	0.18	0.20	0.20

TABLE IX.—COMPARISON OF DATA WITH ANALYSIS FOR 32-DIAMETER SPACING

(a) Liquid: $T_{r,0} = 0.68$; $P_{r,0} = 1.5$

N	$\frac{4fL}{D}$	$\frac{\dot{w}}{\dot{w}_I}$	$\frac{G_r}{G_{r,I}}$ (data)	G_r
1	1.83	0.62	0.6	0.7
2	3.66	.51	.52	.61
3	5.49	.44	.38	.45
4	7.3	.39	.34	.40

(b) Gas: $T_{r,0} = 2.29$; $P_{r,0} = 1.5$

1	0.93	0.69	0.86	0.18
2	1.86	.61	.67	.14
3	2.79	.55	.55	.115
4	3.7	.51	.50	.105

TABLE X.—SOME FRICTION LAWS FOR PIPE FLOW

Laminar	$4f = \frac{64}{\mathrm{Re}}$
Turbulent:	
Blasius	$4f = 4\left(\frac{0.0791}{\mathrm{Re}^{1/4}}\right)$
Smooth tube	$\frac{1}{\sqrt{4f}} = -0.8 + 2\log_{10}(\mathrm{Re}\sqrt{4f})$
Rough tube	$\frac{1}{\sqrt{4f}} = 1.74 + 2\log_{10}\left(\frac{\epsilon}{D}\right)$
Transition	$\frac{1}{\sqrt{4f}} = -2\log_{10}\left(\frac{\epsilon/D}{3.7} + \frac{2.51}{\mathrm{Re}\sqrt{4f}}\right)$

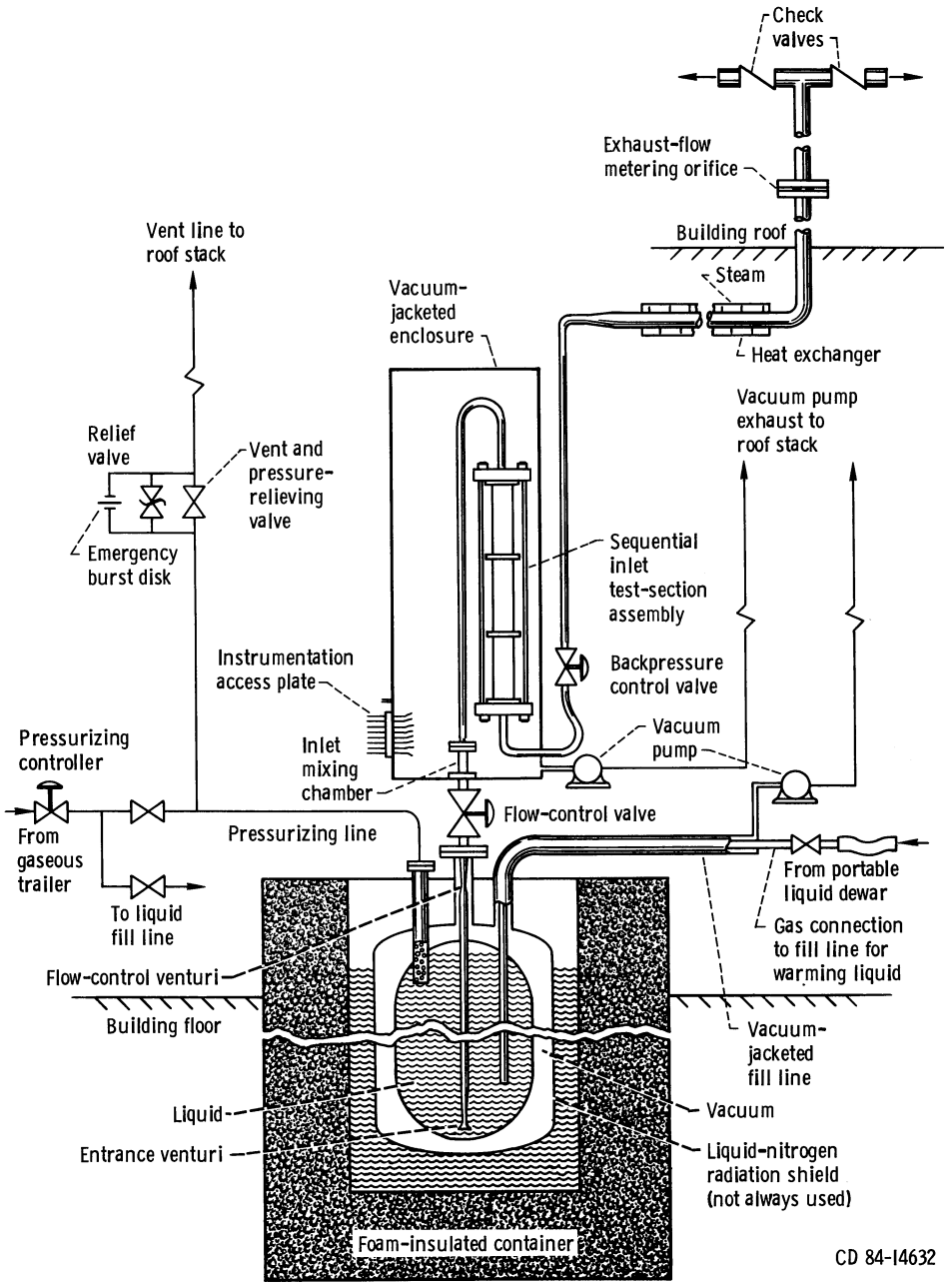

Figure 1.—Schematic diagram of high-pressure liquid flow apparatus with sequential orifice inlet configuration.

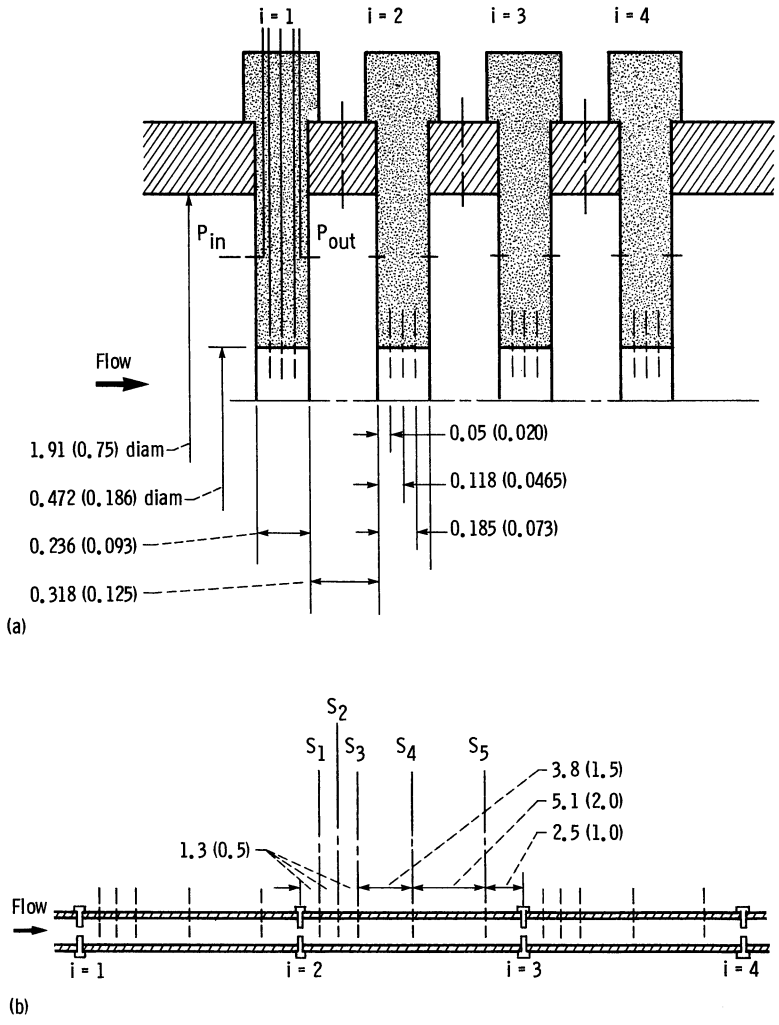

(a) 0.32-cm (0.125-in.) spacer. (b) 15.24-cm (6.0-in.) spacer.

Figure 2.—Schematic of four-sequential-orifice-inlet test section showing axial pressure tap locations on spacers.

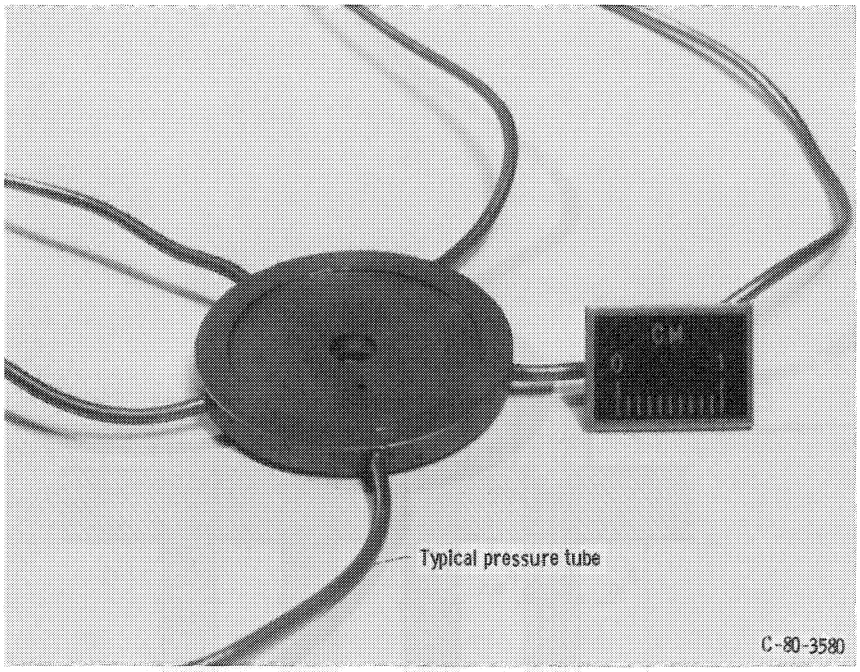

Figure 3.—Orifice inlet.

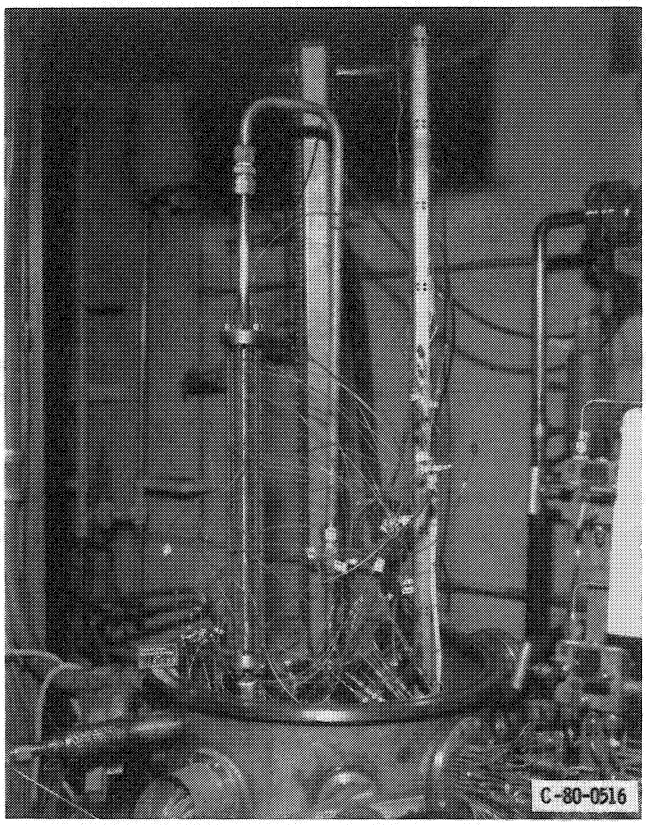

Figure 4.—Installation of four-sequential-orifice-inlet test section with 15.24-cm (6.0-in.) spacer.

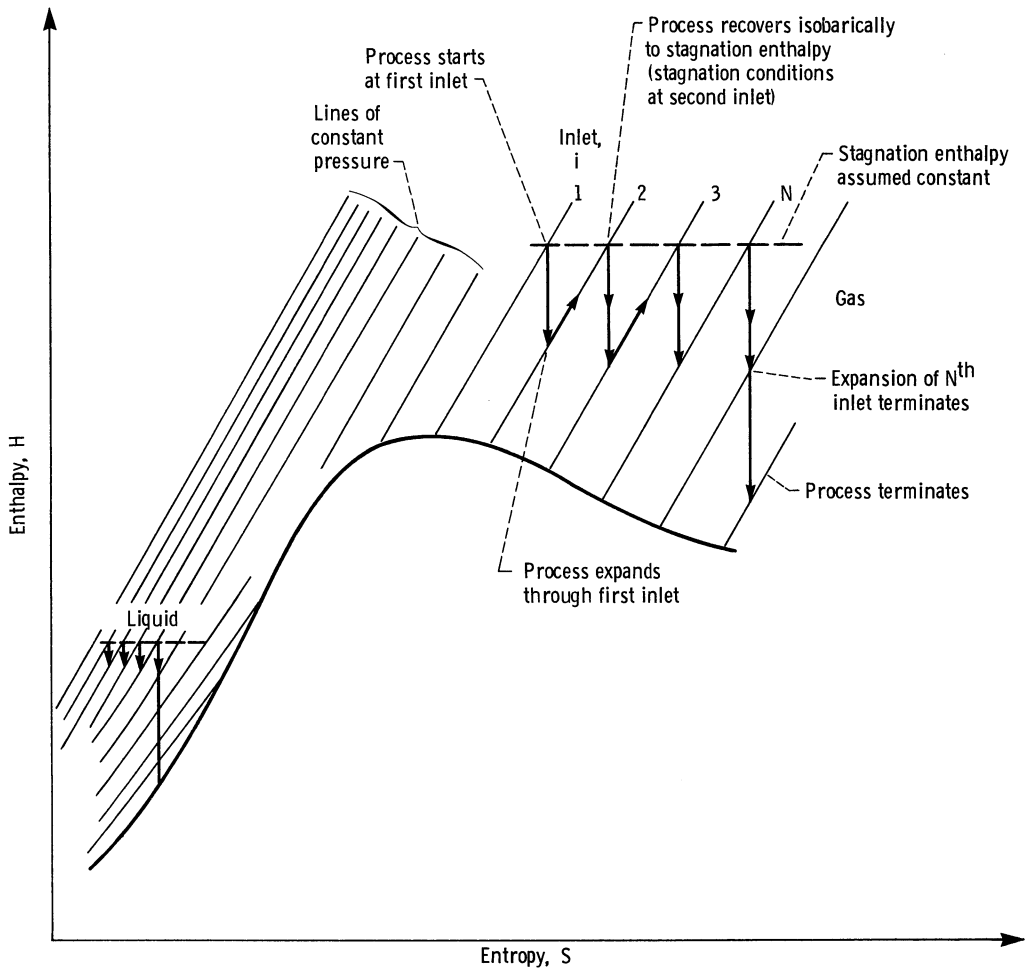

Figure 5.—Process path on an entropy-enthalpy diagram for *N*-sequential-inlet configuration.

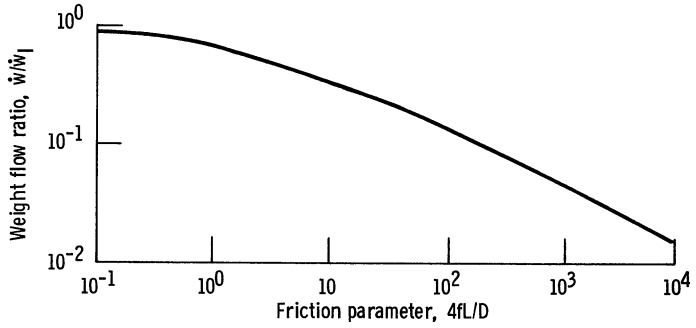

Figure 6.—Ratio of experimental flow to isentropic flow as a function of friction parameter.

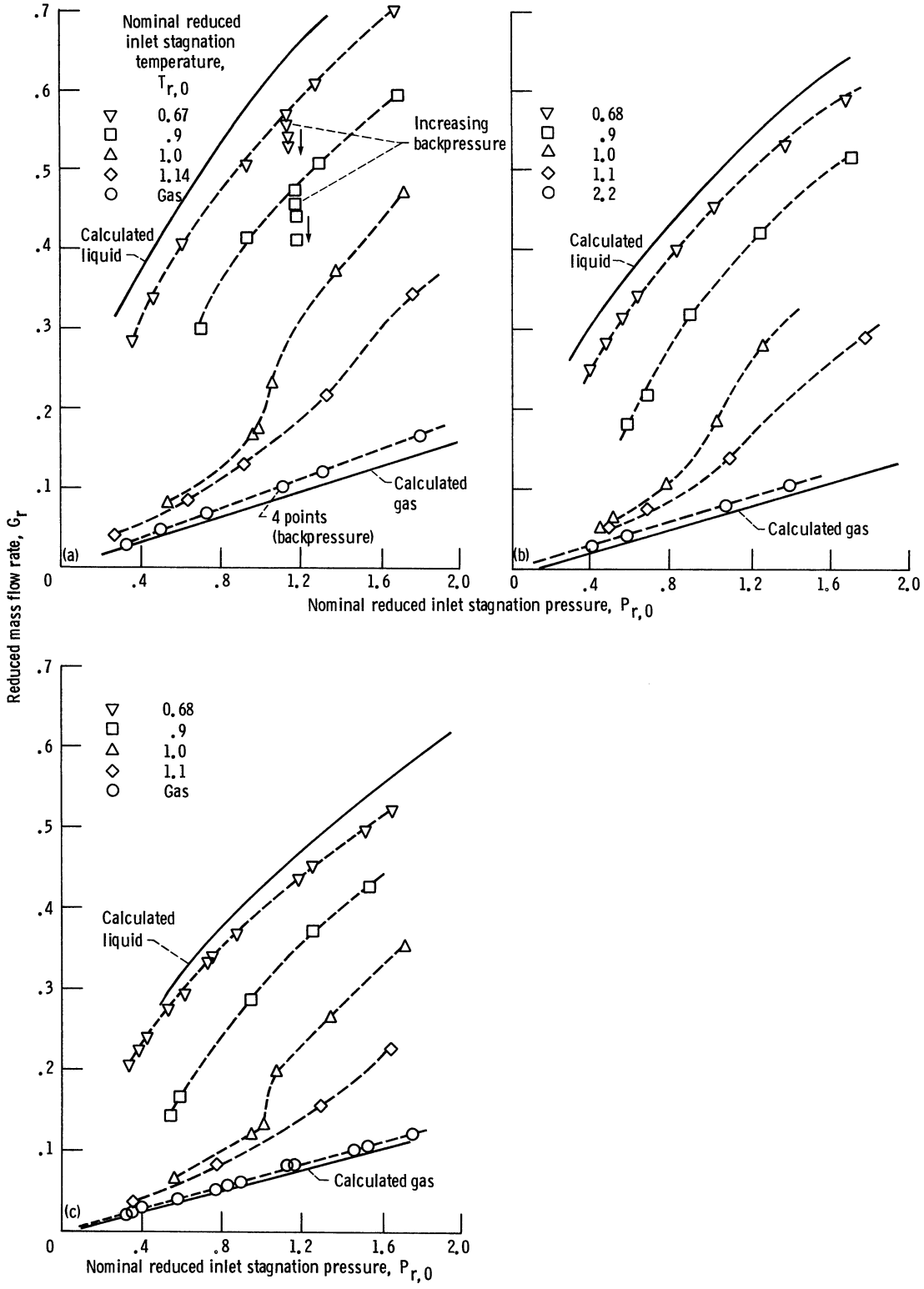

(a) Two orifice inlets at 15.24-cm (6.0-in.) spacing.
(b) Three orifice inlets at 15.24-cm (6.0-in.) spacing.
(c) Four orifice inlets at 15.24-cm (6.0-in.) spacing.

Figure 7.—Reduced mass flow rate as a function of reduced inlet stagnation pressure for selected reduced inlet stagnation temperatures.

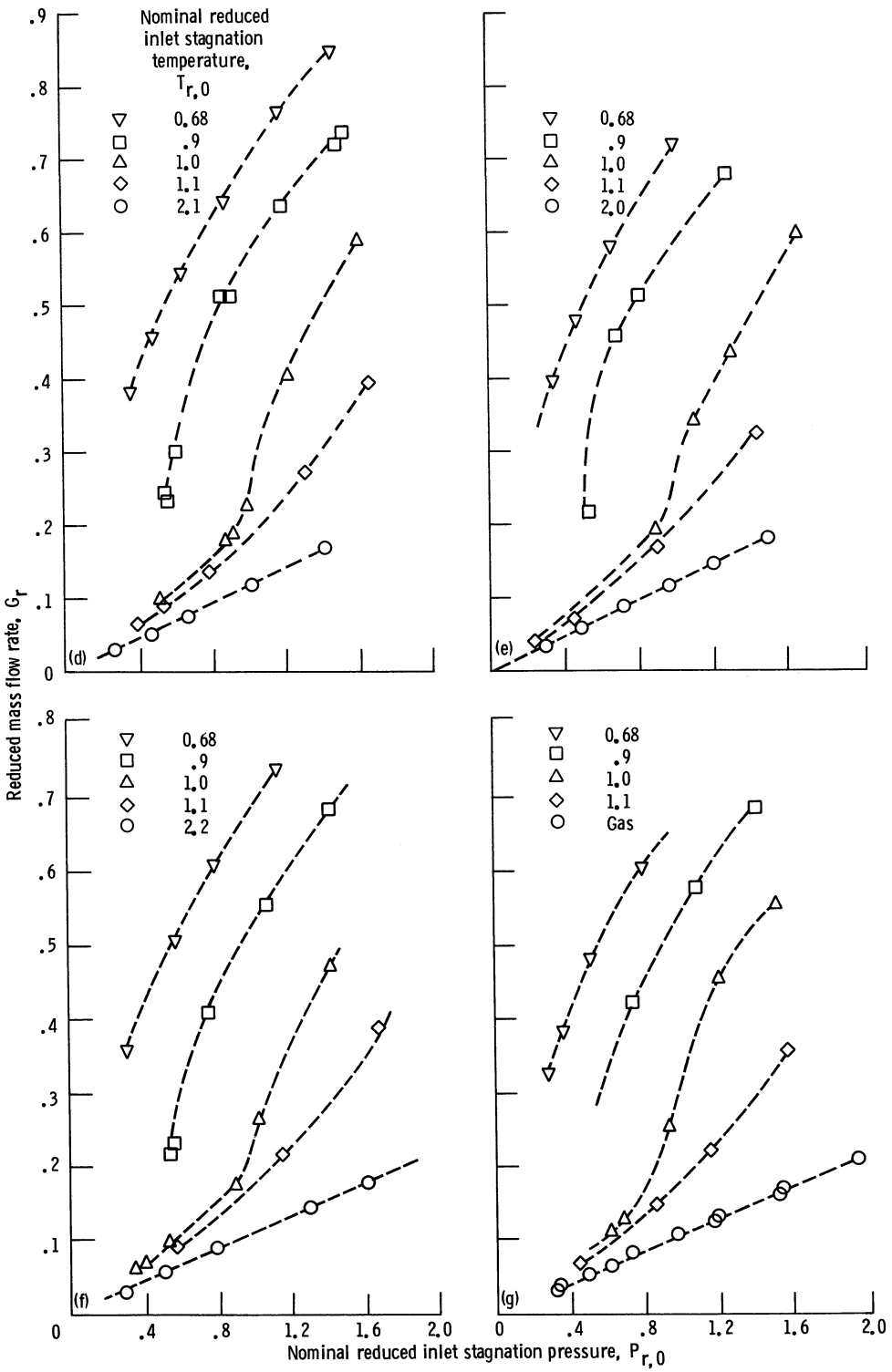

(d) Single orifice inlet.
(e) Two orifice inlets at 0.32-cm (0.125-in.) spacing.
(f) Three orifice inlets at 0.32-cm (0.125-in.) spacing.
(g) Four orifice inlets at 0.32-cm (0.125-in.) spacing.

Figure 7.—Concluded.

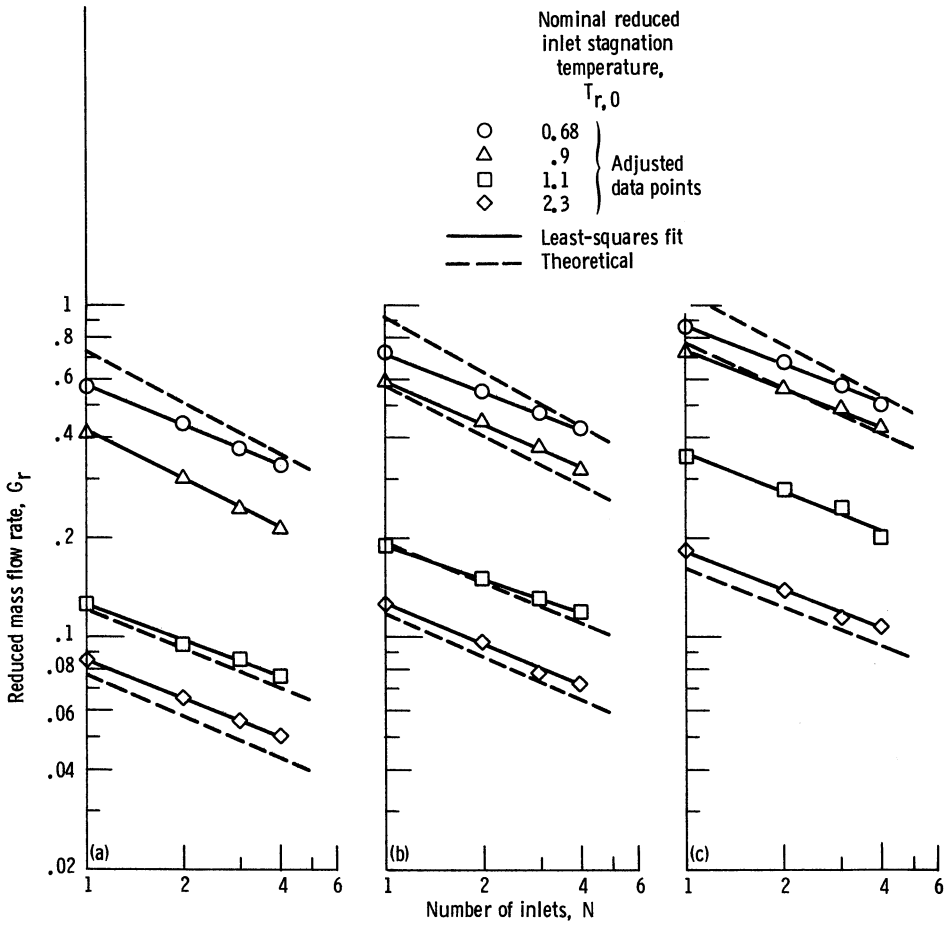

(a) $P_{r,0} = 0.7$.
(b) $P_{r,0} = 1.0$.
(c) $P_{r,0} = 1.5$.

Figure 8.—Reduced mass flow rate as a function of number of inlets for selected reduced inlet stagnation temperatures and reduced stagnation pressures. 15.24-cm (6.0-in.) spacing.

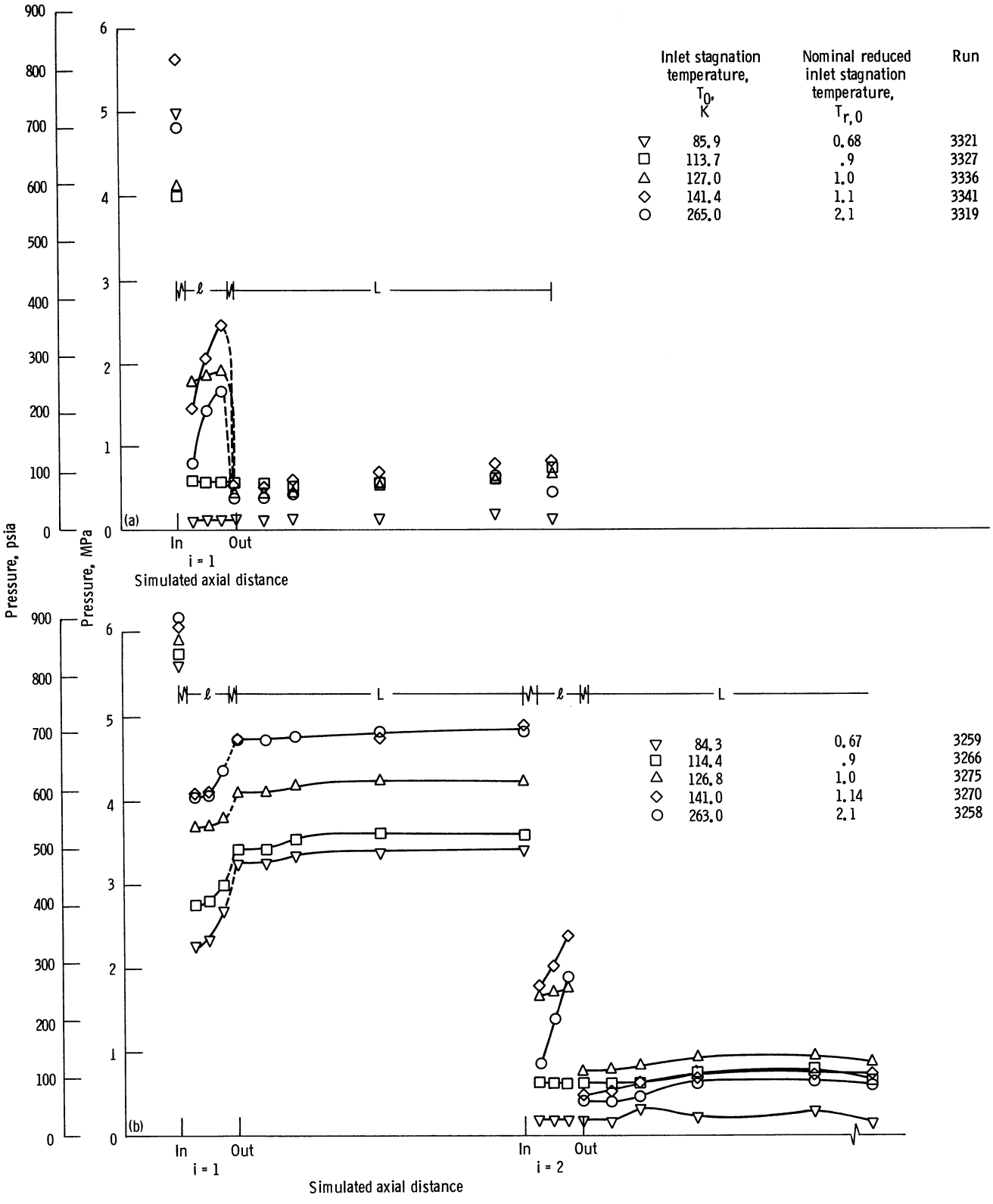

(a) Single orifice inlet.
(b) Two orifice inlets at 15.24-cm (6.0-in.) spacing.

Figure 9.—Pressure profiles at selected inlet stagnation temperatures.

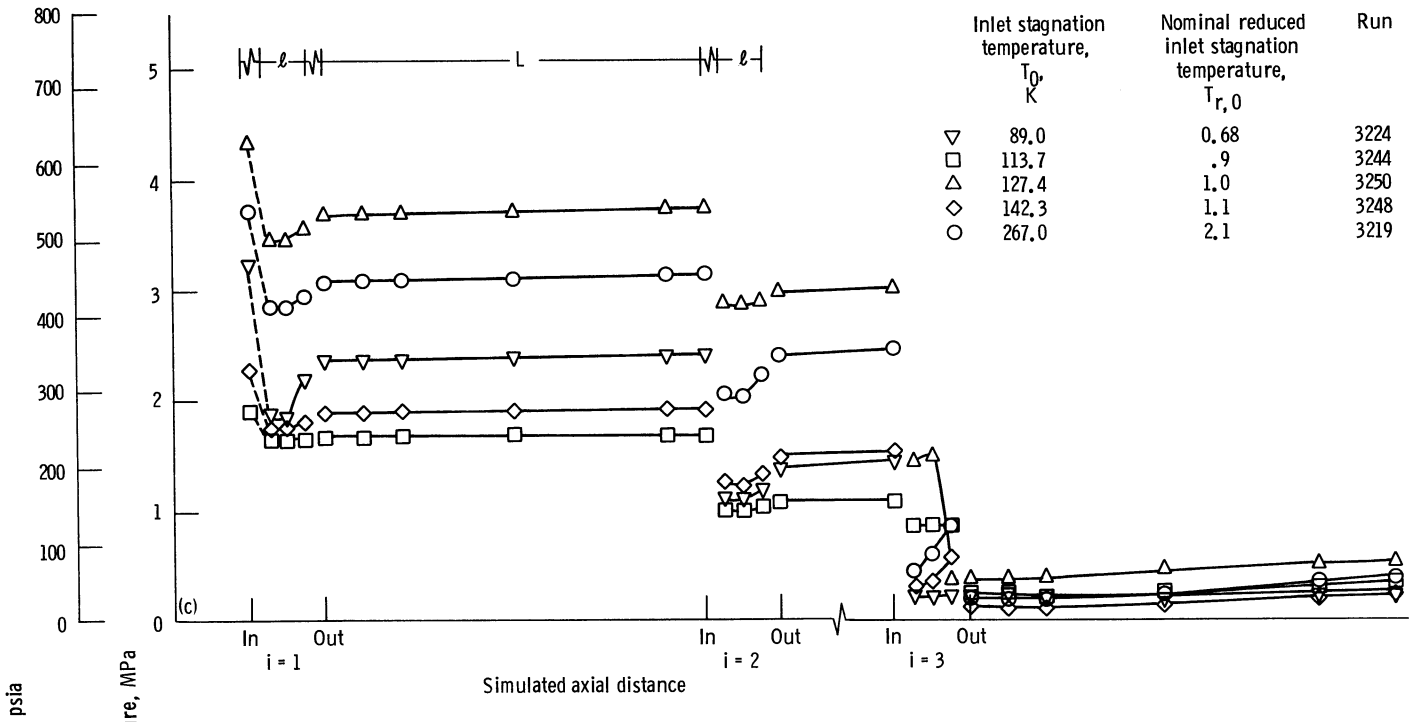

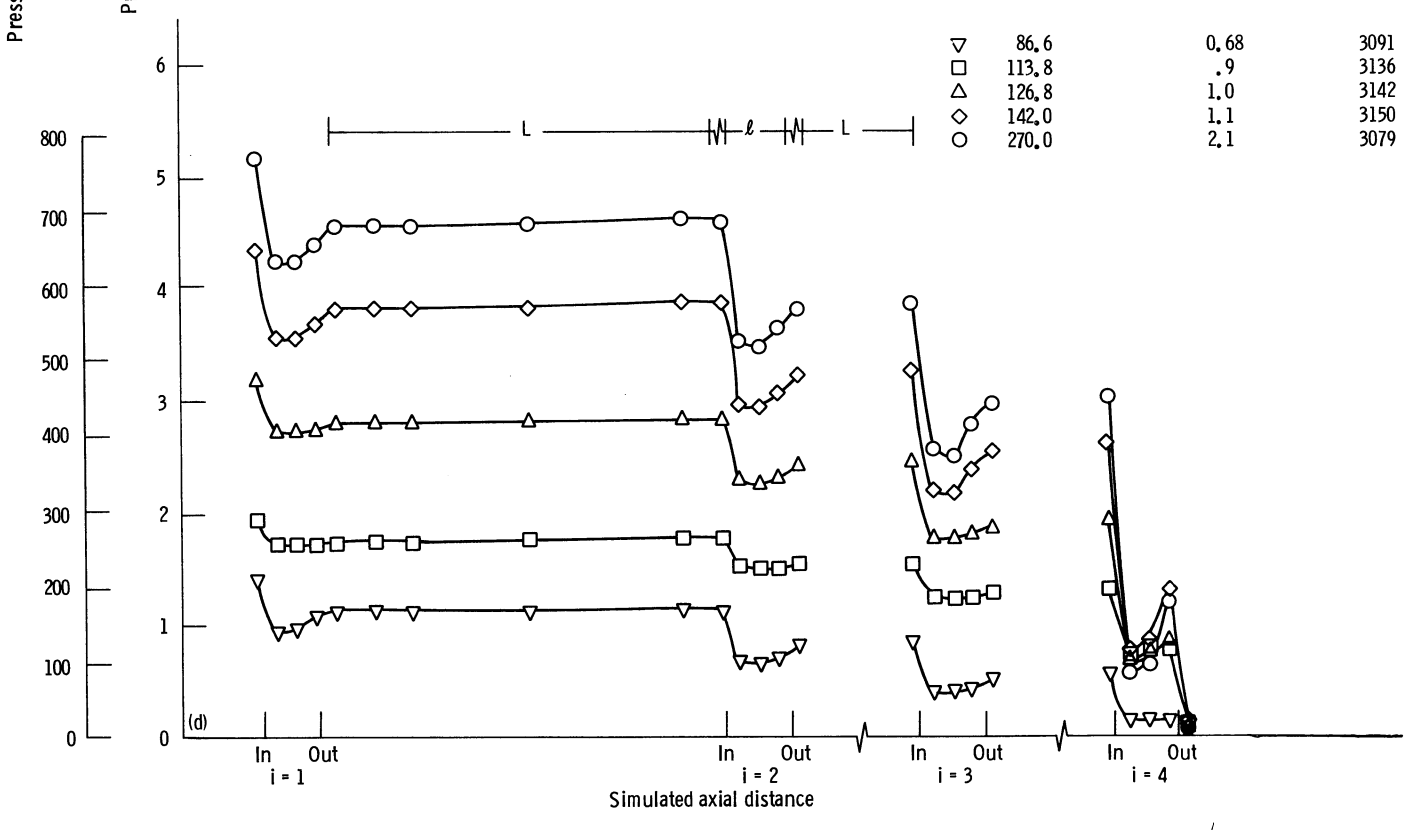

(c) Three orifice inlets at 15.24-cm (6.0-in.) spacing.
(d) Four orifice inlets at 15.24-cm (6.0-in.) spacing.

Figure 9.—Continued.

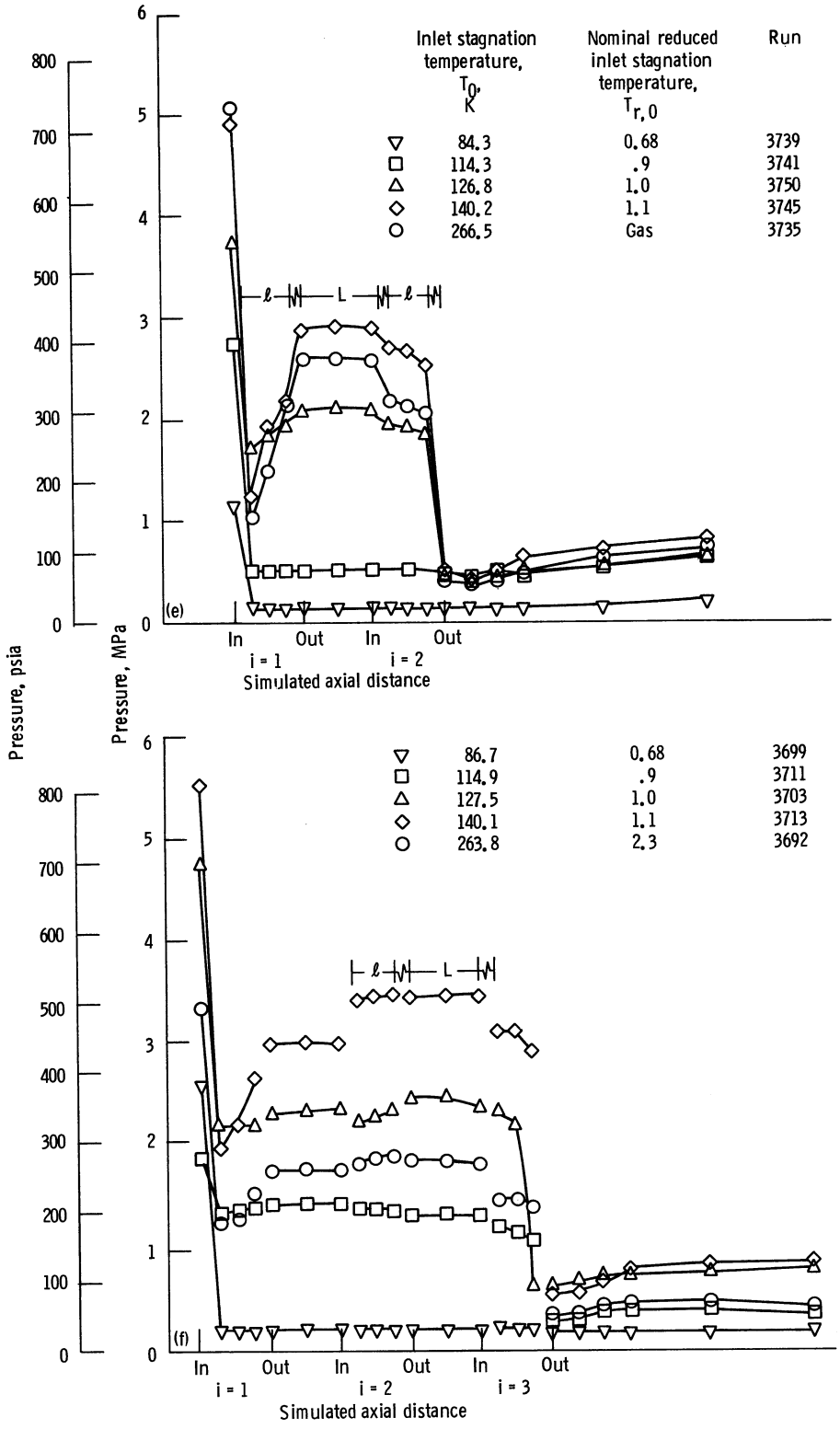

(e) Two orifice inlets at 0.32-cm (0.125-in.) spacing.
(f) Three orifice inlets at 0.32-cm (0.125-in.) spacing.

Figure 9.—Continued.

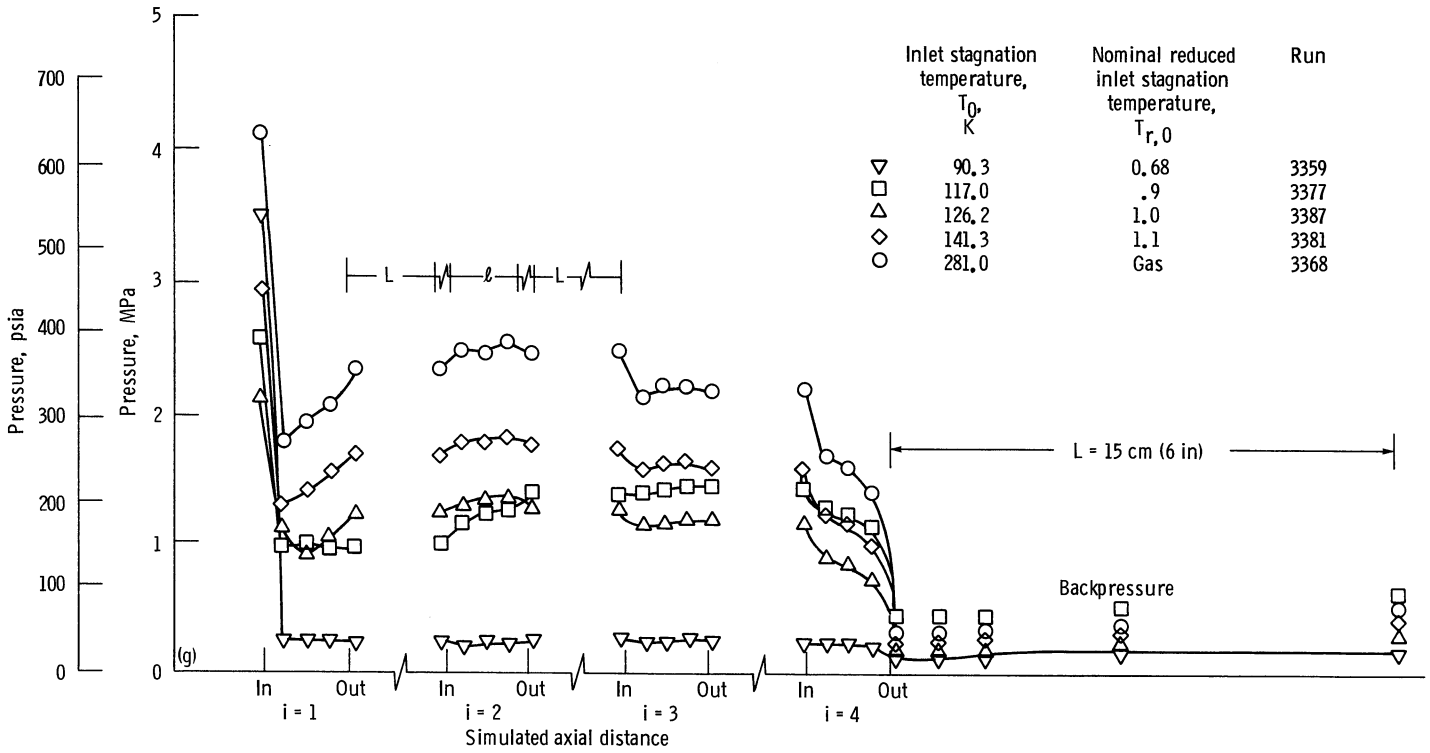

(g) Four orifices at 0.32-cm (0.125-in.) spacing.

Figure 9.—Concluded.

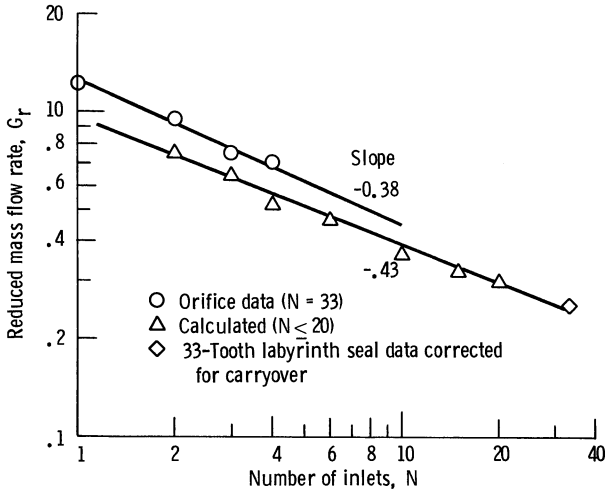

Figure 10.—Reduced mass flow rate as a function of number of inlets, showing slope *b*.

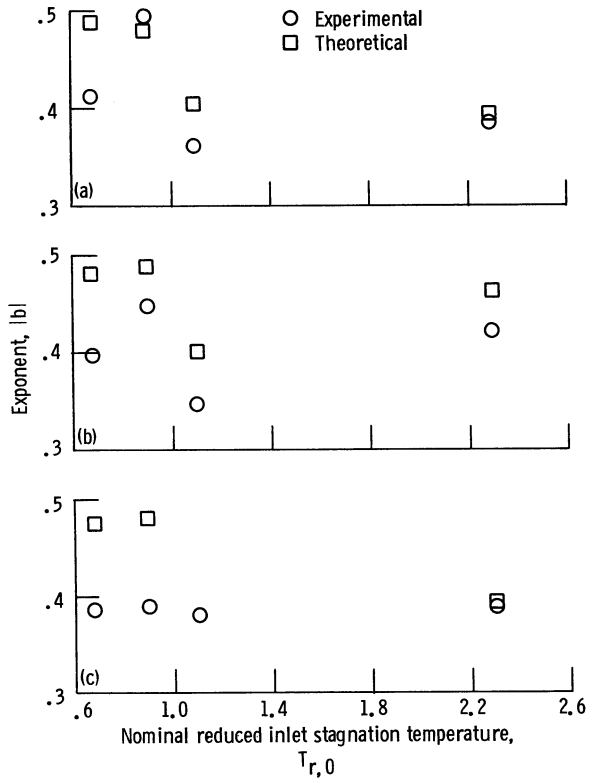

(a) $P_{r,0}=0.7$.
(b) $P_{r,0}=1.0$.
(c) $P_{r,0}=1.5$.

Figure 11.—N^{th}-inlet exponent b as a function of reduced inlet stagnation temperature for selected reduced inlet stagnation pressures. $G_r/G_{r,1}=N^{-b}$.

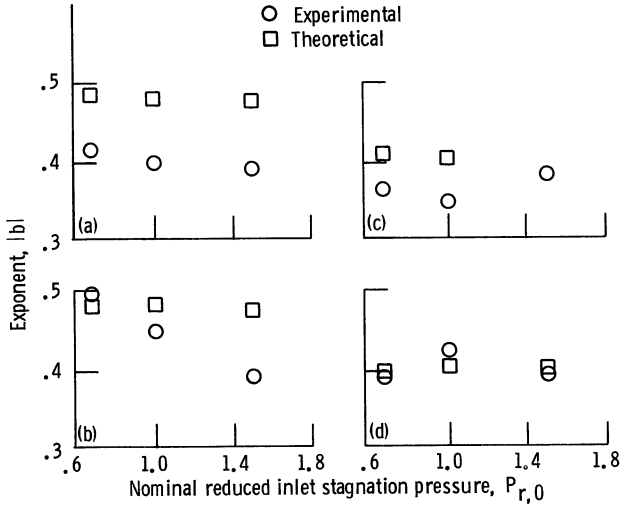

(a) $T_{r,0}=0.68$.
(b) $T_{r,0}=0.9$.
(c) $T_{r,0}=1.1$.
(d) $T_{r,0}=2.3$.

Figure 12.—N^{th}-inlet exponent b as a function of reduced inlet stagnation pressure for selected reduced inlet stagnation temperatures. $G_r/G_{r,1}=N^{-b}$.

1. Report No.	2. Government Accession No.	3. Recipient's Catalog No.
NASA TP-2460		

4. Title and Subtitle	5. Report Date
Flow Rate and Pressure Profiles for One to Four Axially Alined Orifice Inlets	May 1985
	6. Performing Organization Code: 505-32-52
7. Author(s)	8. Performing Organization Report No.
Robert C. Hendricks and T. Trent Stetz	E-1980
	10. Work Unit No.
9. Performing Organization Name and Address	11. Contract or Grant No.
National Aeronautics and Space Administration Lewis Research Center Cleveland, Ohio 44135	13. Type of Report and Period Covered: Technical Paper
12. Sponsoring Agency Name and Address	14. Sponsoring Agency Code
National Aeronautics and Space Administration Washington, D.C. 20546	

15. Supplementary Notes

16. Abstract

Choked flow rate and pressure profile data were taken on sequential axially alined inlets of the orifice type, with an ℓ/d (orifice length-to-diameter ratio) of 0.5. The configuration consisted of two to four inlets spaced at 0.66 and 32 orifice diameters apart. Reference data were taken for the limiting case of a single orifice inlet. At a spacing of 32 diameters the reduced flow rate appeared to follow the simple power-law relation $G_r/G_{r,1} = N^{-b}$, where $G_{r,1}$ is the reduced flow rate for a single inlet, N is the number of inlets, and b, although temperature dependent, is approximately 0.4. At this spacing the instrumented orifices and spacers gave pressure profiles that dropped sharply at the entrance and partially recovered within each inlet, somewhat independent of N. At low inlet temperature jetting through the last orifice was common. At a spacing of 0.66 diameter fluid jetting through all N inlets was prevalent at low temperatures for each configuration studied, as indicated by the flat pressure profiles and flow rates that were nearly identical to those for a single orifice inlet. A simplifying relation was developed between the friction loss parameters for flow through N sequential tubes and N sequential inlets. The predicted flow rates for N tubes were in reasonable agreement with the N inlet analysis and followed the simple power-law relation. Other relations derived from the N-inlet analysis were applied to the experimental flow rates with some success.

17. Key Words (Suggested by Author(s))	18. Distribution Statement
Inlet; Orifice; Sequential flow rate; Pressure profiles	Unclassified - Unlimited STAR Category 34

19. Security Classif. (of this report)	20. Security Classif. (of this page)	21. No. of pages	22. Price
Unclassified	Unclassified	41	A03

For sale by the National Technical Information Service, Springfield, Virginia 22161 NASA-Langley, 1985